CODA-Q ANALYSIS AT MT. ST. HELENS AND ITS IMPLICATIONS FOR VOLCANIC SEISMOLOGY

by

Dai Cole McClurg

A thesis submitted in partial fulfillment
of the requirements for the degree of

Master of Science

University of Washington

1987

Approved by Stephen D. Malone
(Chairperson of Supervisory Committee)

Program Authorized
to Offer Degree Geophysics Program

Date 3-24-87

Master's Thesis

In presenting this thesis in partial fulfillment of the requirements for a Master's degree at the University of Washington, I agree that the Library shall make its copies freely available for inspection. I further agree that extensive copying of this thesis is allowable only for scholarly purposes, consistent with "fair use" as prescribed in the U.S. Copyright Law. Any other reproduction for any purposes or by any means shall not be allowed without my written permission.

Signature_____

Date _____

University of Washington

Abstract

CODA-Q ANALYSIS AT MT. ST. HELENS AND ITS IMPLICATIONS FOR VOLCANIC SEISMOLOGY

by Dai Cole McClurg

Chairperson of the Supervisory Committee: Professor Stephen D. Malone
Geophysics Program

Seismograms of earthquakes located at shallow depth (0 to 10 km) directly beneath or within Mt. St. Helens (MSH) were used to calculate coda-Q, and thereby estimate the attenuation of seismic waves, using the coda-decay method. There are two important results from the coda-Q analysis at MSH. First, the coda-Q values corresponding to a small shallow volume of rock including the volcano are an order of magnitude lower than the coda-Q values corresponding to a much larger volume of rock surrounding the volcano. Second, the coda-Q values corresponding to a shallow volume of rock including the volcano are slightly lower than the values corresponding to a slightly deeper volume of rock including the volcano. These two coda-Q results indicate that Q is lower at MSH than it is in the surrounding crust. A simple model for this spatial variation of Q, or "Q-structure", which is consistent with the above results consists of a small hemispherical volume of rock surrounded by rock with a higher Q. This model was used to correct the spectra of the codas of volcanic seismograms for attenuation. The spectral observations are consistent with two statements about volcanic earthquakes. First, the cause of the relatively low frequency coda of medium frequency volcanic earthquakes is the Q-structure at MSH rather than a hypothetical non-tectonic source. Second, low frequency volcanic earthquakes have a source which is different than a typical tectonic source, at least in terms of source duration.

TABLE OF CONTENTS

LIST OF FIGURES

LIST OF TABLES

ACKNOWLEDGEMENTS

Many people have helped me during the course of this project. Jens Havskov, from the University of Bergen in Norway, provided the software for the analysis as well as some crucial and timely guidance. Throughout my graduate work, Tony Qamar has offered me help and advice, and I am very grateful to him. Steve Malone provided the project and several helpful pep-talks. Bob Crosson made some helpful suggestions and reviewed this thesis. My friends and office mates, Rob Leet and Peggy Browne, have been a constant source of cheer and camaraderie and this project would have been much more difficult without them. I am "eternally indebted" to Rick Benson who provided a great deal of help handling seismic data and making the computers cooperative. Tom Yelin's words of wisdom allowed me to develop the proper perspective. Finally, I would like to thank Ron Merrill for his advice throughout my graduate work.

CHAPTER I

INTRODUCTION

In March of 1980, Mt. St. Helens (MSH) resumed its eruptive activity after a dormant period beginning in 1857 (Mullineaux and Crandell, 1981). Most of the seismic activity at MSH occurs immediately before, during, and immediately after eruptions. Since May 17 of 1980 twenty three eruptions have occurred and the seismograms of thousands of volcanic earthquakes have been recorded. The seismograms display a broad spectrum of characteristics (see figure 1.1). The purpose of this study is to demonstrate that some of the principal characteristics of these seismograms are due to the attenuation of seismic waves in the earth's crust.

Seismic signals at MSH are produced by both surface and subsurface processes. Mudflows and avalanches are examples of surface processes that produce such signals. During eruptions of ash and steam, there are accompanying signals which originate at shallow depth. However, the majority of the seismic signals have entirely subsurface sources. These signals are referred to as "volcanic earthquakes" and their seismograms are called "volcanic seismograms". At one end of the spectrum there are seismograms which are identical to those of tectonic earthquakes. At the other extreme are seismograms which are unique to volcanoes. These are the so-called "low frequency" or "B-type" seismograms (Minakami, 1960). Intermediate between the two extreme types are the "medium frequency" seismograms. Numerous attempts have been made to explain the reasons for the diversity of seismic signals produced by subsurface sources at volcanoes, and MSH in particular.

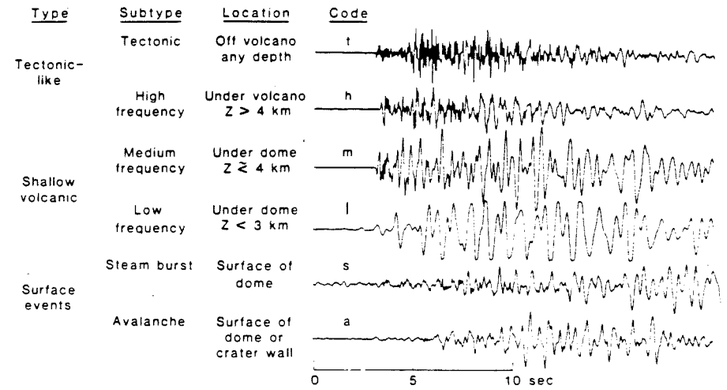

Fig. 1. Characteristic seismograms for the six categories of events observed at Mount St. Helens. Seismograms are from station SHW, located 3.6 km west of the active dome. The example of type t is from a tectonic earthquake located 8.2 km south of the dome at a depth of 5.6 km; type h, a high-frequency volcanic earthquake located under the dome at a depth of 6.2 km. The remaining four events occurred at shallow depth or at the surface near the dome: the example of type m is from a medium-frequency volcanic earthquake; type l, a low-frequency volcanic earthquake; type s, an observed gas burst from the top of the dome; type a, a rock avalanche from the south crater wall.

Figure 1.1 Examples of seismic signals at Mt. St. Helens. All seismograms are from the same station (from Malone et al., 1983).

An important motivation for understanding these subsurface sources is the desire to use seismic monitoring for eruption prediction.

A seismogram is the result of several factors. One factor is the nature of the earthquake source. One hypothesis is that the diversity in the volcanic seismograms is due to a diversity of source mechanisms. Several authors have proposed source models for the more unusual volcanic earthquakes (e.g. Chouet, 1985). Another contribution to the characteristics of volcanic seismograms is the medium through which the seismic waves propagate. The effects of the medium on seismic wave amplitudes are called "path-effects". The path-effect that is the focus of this thesis is the attenuation of seismic waves. The parameter that is used to describe the attenuation is the quality factor, or "Q". The degree of attenuation is inversely proportional to Q. One way to measure Q from a seismogram is the "coda-decay method" which was developed by Aki and Chouet (1975). The resulting values of Q are called "coda-Q" values.

There are two important results from the coda-Q analysis at MSH presented here. First, the coda-Q values corresponding to a small shallow volume of rock near (and including) the volcano are much lower than the coda-Q values corresponding to a much larger volume of rock surrounding the volcano. Second, the coda-Q values corresponding to a shallow volume of rock near (and including) the volcano are slightly lower than the values corresponding to a slightly deeper volume of rock near (and including) the volcano. These two coda-Q results indicate that Q is lower at MSH than it is in the surrounding crust. A simple model for this spatial variation of Q, or "Q-structure", which is consistent with the above coda-Q results, was proposed and calculated. This model was used to attempt to separate the effects of source and path on the seismograms of volcanic earthquakes. Specifically,

it was used to correct for the effect of attenuation on the spectra of the codas of volcanic seismograms. The effect of the Q-structure on the spectral content of volcanic seismograms is significant and any explanation for the diversity of volcanic seismograms at MSH must account for the effect of this Q-structure. The spectral observations are consistent with two statements about volcanic earthquakes. First, the cause of the relatively low frequency coda of medium frequency volcanic earthquakes is the Q-structure at MSH rather than a hypothetical non-tectonic source. Second, low frequency volcanic earthquakes have a source which is different than a typical tectonic source, at least in terms of source duration.

CHAPTER II

VOLCANIC EARTHQUAKES

Many of the active volcanoes in the world produce seismic signals with dominant periods ranging from about 1 second ("low-frequency") to 0.05 seconds ("high-frequency"). Volcanic tremor is a type of low-frequency signal which has a duration of many minutes to hours. Tremor is thought to be directly related to the movement of magma or other fluids beneath and within a volcano (e.g., Aki and Koyanagi, 1981). All of these signals are observed at Kilauea in Hawaii (Aki and Koyanagi, 1981), Pavlov volcano in Alaska (McNutt, 1986), and MSH (Malone, 1983). In a few cases, certain types of signals can be correlated with visually observable phenomena at the surface such as explosions (McNutt, 1986), fountains, or steam emissions. These signals can be readily associated with an observed source process. The majority of seismic signals at MSH have subsurface sources so that it is necessary to use the seismograms to indirectly infer the characteristics of the sources. The first step in using seismograms for this purpose is the development of a scheme to unambiguously classify different types of seismograms.

The seismic signals at MSH which have subsurface sources range from the high frequency type (h) to the low-frequency type (l) (see figure 1.1). Volcanic tremor is also observed at MSH. Malone and Qamar (1985) proposed that tremor is directly related to the type (l) events. Chouet (1985) proposed that the type (l) events are the impulse response of a tremor generating system and that tremor is constituted by a continuous sequence of type (l) events. The very long duration and non-decaying amplitude of

tremor suggests that the duration of the tremor source is much longer than a typical tectonic source. A short duration source is assumed in the theoretical development of the method which is used to calculate coda-Q in this study. Therefore, tremor was not used in any of the calculations and it will not be discussed in the classification scheme below. However, by discussing the type (l) events, we may be discussing a type of signal directly related to tremor.

Types of Volcanic Seismograms

The following scheme was developed and used at the University of Washington for MSH earthquakes. It was developed primarily for the purpose of predicting eruptions by observing changes in the type of waveforms recorded at particular stations located on MSH. The following types of seismograms are recorded by these stations. The hypocenters for all of these event types are located directly beneath or within the volcanic structure (Malone, 1983; Malone et al., 1983)

Type (h). High frequency seismograms (h) have hypocenters located at depths greater than 3 kilometers. These seismograms are very similar to typical tectonic earthquake seismograms but are somewhat depleted in high frequency energy compared to a tectonic seismogram. They have impulsive and clear P and S phases and focal mechanisms which are consistent with the tectonic environment in the vicinity of the volcano (Weaver et al., 1981). In addition, when type (h) events are recorded by stations away from the volcano their seismograms, and the spectra calculated from them, are negligibly different from tectonic seismograms and their spectra (Malone, 1983). These observations suggest that (h) events have normal tectonic sources (shear

failure on a fault) and that the slight depletion of high frequency energy is due to path effects (attenuation) within the volcanic structure.

Type (m). Medium frequency earthquakes have focal depths from 3.0 km to the surface. Their seismograms have clearly impulsive first arrivals but lack a clear S phase and have a low frequency coda compared to the early part of the seismogram. The spectra of these seismograms (uncorrected for attenuation) have a dominant peak at frequencies higher than two hertz at all stations. For a given earthquake the exact frequency at which this peak occurs varies from station to station suggesting that path effects, rather than source effects, are controlling the location of this peak.

Type (l). Low frequency earthquakes (l) have focal depths in the same range as type (m) events. Their seismograms have very emergent first arrivals, no clear phases, and a low frequency, almost monochromatic looking form. The spectra of low frequency seismograms (uncorrected for attenuation) are strongly peaked at about 1 Hz at all stations. Fehler and Chouet (1982) argue that the invariance of the location of this spectral peak with earthquake magnitude indicates that the peak is due to a source effect rather than a path effect.

Both type (l) and (m) events have locations which are concentrated in a shallow volume roughly 2 km in horizontal radius centered on the dacite dome in the crater. The similarity of the locations of the sources for (l) and (m) events suggests that path effects are not the dominant cause of the difference between the seismograms for these events. Rather it seems that the difference must be due largely to differences in the sources themselves.

Causes of the Diversity of Volcanic Seismograms

The above classification scheme is based on the observed seismograms at a given station on the volcano. The seismograms of a given event appear significantly different at different stations in terms of dominant frequency and impulsiveness suggesting that path effects and site effects have a significant influence on the nature of volcanic seismograms. There is a direct correlation between depth of focus and waveform type. Shallower sources tend to have lower dominant frequencies. Malone (1983) proposes two extreme explanations for this effect. The first assumes that wave-path effects are dominant and the second assumes that source effects are dominant.

Path Effects. In the first explanation, the sources are assumed to be similar at all depths so that the changes in the seismograms are due to the location of the source within a medium which has properties that change with depth. In other words, as the sources become more shallow they leave the regional tectonic environment and enter the volcanic structure. The volcano is composed of materials with different properties than the surrounding crust. There is a great deal of velocity contrast in the shallow structure indicating that the volcano has a complicated velocity structure. The observed P-wave velocity near MSH ranges from 0.42 km/sec in loose pumice at the surface, to 3.2 km/sec in old lava flows, 4.8 km/sec in old sedimentary rocks, and 6.0 km/sec in the crystalline basement (Weaver and Malone, 1976). The low-velocity near-surface materials, such as pyroclastic rocks, should have a higher anelastic attenuation (Weaver, 1976). In addition, the volcano is composed of a heterogeneous combination of low and high velocity materials. Heterogeneities in a medium cause scattering of seismic waves which increases seismic wave attenuation. It is possible that the lack of an S-phase

for the impulsive type (m) seismograms is caused by strong scattering of S-waves within the heterogeneous medium of the volcano.

The above observations suggest that attenuation due to anelastic attenuation and scattering may be high within the volcano, possibly higher than in the deeper crust beneath the volcano. This type of structure, combined with a single type of source, could cause or contribute to the observed "source depth effect". In other words, as the tectonic type source (shear failure on a fault) leaves the deeper, less attenuating materials and enters the shallow highly attenuating medium of the volcano, the resulting seismograms become relatively depleted in high-frequency energy. This hypothesis is consistent with observations of type (m) events. However, as we will see in chapter VIII, it is difficult to explain the emergent low-frequency earthquakes in terms of a typical tectonic source.

Source Effects. The other extreme explanation for the source depth effect attributes the correlation between depth and waveform type to source mechanisms which change with depth. For example, the type (h) events may be the result brittle shear failure, while the type (l) events may be the result of a different type of source which is unique to volcanoes. Many different types of source mechanisms have been proposed for the type (l) seismograms and tremor at MSH and other volcanoes. Crosson and Bame (1985) proposed a source composed of an oscillating gas bubble enclosed in magma surrounded by country rock. St. Lawrence and Qamar (1979) proposed a hydraulic transient mechanism. Aki et al. (1977) proposed a fluid driven crack mechanism. Some of these mechanisms may not be appropriate for MSH since they were used to model sources from volcanoes which erupt basaltic lavas, which are less viscous than the dacite magma at MSH.

Remarks. Malone (1983) argues that the source depth effect at MSH cannot be explained by either path effects or source effects alone. The goal of this thesis is to quantify the effect of attenuation at MSH so that the effects of path and source can be separated. My coda-Q results indicate that the attenuation of seismic waves is higher at MSH than in the underlying crust and that the source depth effect is partly caused by this Q-structure. The spectral results in chapter VIII suggest that the source of a typical type (m) earthquake is significantly different from the source of a type (l) event. Thus, the source depth effect is a combination of path and source effects. The Q-structure indicated by the coda-Q results of this thesis provides an important constraint on explanations for the diversity of seismic signals recorded at MSH and suggests the need for similar studies at other volcanoes.

CHAPTER III

CODA THEORY

As seismic waves travel through a medium their amplitude diminishes. The two causes for this decreasing amplitude are geometrical spreading and attenuation. Geometrical spreading is independent of frequency and given the types of waves involved (surface or body) and a velocity model, one can easily account for it. However, the attenuation is a function of frequency and depends on the properties of the medium (other than velocity) through which the waves propagate. Thus, the decreasing amplitude of seismic waves as they travel away from the source is a measure of the properties of the medium along the wave path. The parameter that is used to describe the attenuation of seismic waves is called Q. There are several ways to measure Q from a seismogram. The two primary methods are the spectral ratio method (eg. Bakun and Bufe, 1975) and the coda decay method (Aki and Chouet, 1975).

The spectral ratio method has been widely used to calculate Q from direct body waves (e.g. Bakun and Bufe, 1975). Usually, the ratio of shear wave spectra is taken from two seismograms of the same earthquake recorded at stations at different distances from the source. The S wave far-field displacement spectrum S may be represented by

$$S(f\ ,t\ ,\theta,\phi) = I(f\ )\ C(f\ )\ \sigma(f\ ,\theta,\phi)\ P(f\ ,t\ )\ R\ (\theta,\phi)$$

where I is the total displacement response of the recording system, $C(f\ )$ is

the free surface response, σ is the spectrum of the source, P accounts for the effect of attenuation, and R is the effect of the radiation pattern. P is taken to have the form

$$P(f, t) = g(t)\, e^{-\pi f t / Q_\beta}$$

where g is the effect of geometrical spreading, f is frequency, t is time since earthquake origin ("lapse time"), and Q_β is the "shear wave Q" and is a measure of the attenuation along the particular direct wave path between the source and receiver (Bakun and Bufe, 1975). When the ratio of the spectra at two different stations is taken then the source spectrum will cancel. If the functions I and R are known then the only unknown quantity in the ratio will be the the value of Q_β. For volcanic seismograms at MSH the spectral ratio method cannot be easily used because I is known for only a few stations, and most of the seismograms recorded on the volcano do not display easily recognizable direct shear wave phases. Is is often impossible to calculate focal mechanisms which means that R cannot be determined.

The coda decay method has become very widely used since it was developed by Aki and Chouet (1975). "Coda-Q" is calculated from the shape of the envelope of the coda (tail) of a seismogram. It is a useful method to use at MSH because it doesn't require knowledge of the recording system response or the radiation pattern.

The values of Q which are measured from a seismogram are due to two independent processes. These are the anelastic attenuation of the medium, which results in the conversion of seismic energy into heat, and the scattering of waves by heterogeneities within the medium, which results in a transfer of energy from the direct waves into the energy of the coda waves (Sato, 1977).

In this way, scattering is thought to diminish the amplitude of both direct and coda waves while it also acts as a source for coda waves.

Aki (1981) concluded that coda waves are S-to-S backscattered waves which is supported by the agreement between estimates of coda-Q and Q_β in a given geographic region (e.g. Aki, 1980; Kvamme, 1985). In addition, the mean site effect for S waves arriving at a given station from earthquakes located at a range of azimuths, is equal to the coda site effect for that station (Herraiz and Espinosa, 1986).

The anelastic attenuation of the medium is described by the parameter Q_i which is called the intrinsic-Q. The attenuation due to scattering is described by the parameter Q_s which is called the scattering-Q. Dainty (1981) showed that the relationship between the measured Q and its two contributions is

$$\frac{1}{Q} = \frac{1}{Q_i} + \frac{1}{Q_s} \qquad (3.1)$$

In order to separate Q_i from Q_s, a model for the scattering process must be specified. Without direct knowledge of the sizes and the number of scatterers involved, it is difficult to specify such a model.

The measured Q is usually a strong function of frequency. It is usually assumed that Q_i is independent of f and that the frequency dependence of the measured Q is due to the scattering process (Dainty, 1981). I made no attempt in this thesis to separate the effects of scattering and anelastic attenuation because it has no direct bearing on the main goal of this thesis which is the separation of path and source effects for volcanic seismograms.

The coda is the tail of a seismogram after the direct P and S waves have decayed. Aki (1969) proposed that the coda is composed of backscattered waves from numerous heterogeneities in the lithosphere. Backscattering is primarily caused by impedence contrasts (Herraiz and Espinosa, 1986). Conceptually, as the direct P and S waves travel through the medium away from the source they encounter heterogeneities which scatter energy back toward the source and receiver, thus leaving behind a pool of scattered energy (the coda) in the vicinity of the source which slowly decays. The way in which the pool decays depends on the type of scattering involved. The two extreme types of scattering are single scattering and diffusion. In the single scattering case, each backscattered wave that arrives at the receiver has encountered no additional scatterers on its way back from the scatterer which produced it. In the Born approximation, only a negligible amount of energy is removed from the direct waves by each scattering encounter (Aki and Chouet, 1975) so that the amplitude of the direct waves is greater than the coda wave amplitude. In the case of diffusion, extreme multiple scattering occurs so that each backscattered wave that arrives at the receiver has encountered many scatterers. The direct waves are quickly converted entirely into scattered waves after traveling only a short distance and the energy density of the pool of scattered waves obeys the diffusion equation (Aki and Chouet, 1975). An example of this process is found on the Moon. The Lunar interior is characterized by intense scattering and negligible anelastic attenuation so that the dominant attenuative process is scattering. Several authors have explained the scattering of Lunar seismic waves as a diffusion process (e.g. Dainty and Toksoz, 1977). For small local earthquakes, single scattering is believed more appropriate than diffusion (Gao et. al., 1983). This belief is supported by fact that the amplitude of the direct waves is usually much larger that the coda wave amplitudes. The farther the direct waves travel

the greater the variety of scatterers they encounter. Therefore, we may assume that the characteristics of the coda are the result of wave superposition caused by scattering from many different heterogeneities. It should then be possible to describe the coda with a small number of statistical parameters which characterize the average properties of the medium (Aki and Chouet, 1975). High-resolution frequency-wave number spectra show that coda energy arrives from all azimuths while the direct P and S waves arrive from one azimuth (Capon, 1969). Thus, the assumption that the coda is composed of backscattered waves from randomly distributed heterogeneities in the lithosphere, made by Aki and Chouet (1975), is supported by the findings of Capon (1969).

Aki and Chouet (1975) derived an expression for the power spectrum of coda waves assuming that the source process for the coda is single backscattering and that the distance between the source and receiver is small compared to the distance traveled by the coda waves. The expression is

$$P(f\ ,\ t) = S(f\ )\ t^{-2u}\ e^{-2\pi f t/Q} \qquad (3.2)$$

where t is lapse time, f is frequency, S represents the effect of the earthquake source and the coda wave sources, t^{-2u} is the correction for geometrical spreading, and Q is coda-Q. The value of u in the geometrical spreading term depends on the type of waves composing the coda, with a value of 1.0 for spherical body waves and 0.5 for surface waves. Equation 3.2 also holds when the coda is waves which have undergone extreme multiple scattering (diffusion). In that case the value of u is 0.75.

Assuming singly backscattered body waves and allowing the distance between the source and receiver to be comparable to the distance traveled by

coda waves, (Sato, 1977) showed that the coda power spectrum is expressed by

$$P(f\ ,\ t) = S(f\ )\ \frac{1}{\alpha}\ ln\ (\frac{\alpha+1}{\alpha-1})\ e^{-2\pi f t/Q} \qquad (3.3)$$

where S is the product of source, site, and backscattering effects (Philips et al., 1986), $\alpha = t/t_s$, and t_s is the direct shear wave travel time. Notice that the difference between equations 3.2 and 3.3 lies in the geometrical spreading term. However, Sato (1977) showed that

$$\frac{1}{\alpha}\ ln\ (\frac{\alpha+1}{\alpha-1}) \approx t^{-2} \qquad (3.4)$$

when the lapse time is greater than $2t_s$. Note that t^{-2} corresponds to $u = 1$. For all of the analysis done at MSH, I have assumed single backscattering of shear waves and the lapse times used are all greater than $2t_s$ so that the geometrical spreading term in the power spectrum was taken to be t^{-2}.

Assuming that the distance between the source and receiver is small compared to the distance traveled by coda waves, (Aki and Chouet, 1975) described the envelope of the coda by the amplitude spectrum

$$A(f\ ,\ t) = C(f\ )\ t^{-u}\ e^{-\pi f t/Q} \qquad (3.5)$$

where A is the amplitude of the envelope of the coda as a function of frequency and lapse time, $C(f\ )$ is the coda-source-factor which is assumed to be independent of f in a narrow frequency band centered on f, u is the

geometrical spreading parameter which is 1.0 for body waves and 0.5 for surface waves, and Q is coda-Q

Equation 3.5 holds for all types of scattering including the extreme cases of single-scattering and diffusion (Aki and Chouet, 1975). The seismograms used to calculate coda-Q in this thesis were divided into two data sets, based on the depths of the earthquake sources (see chapter VI). For the shallow data set the distance between the sources and receivers is small compared to the distances traveled by coda waves. Thus, equation 3.5 holds for this data since a zero source-receiver distance was assumed in its derivation. For the deep data set, however, the sources have depths which are comparable to the distances which are traveled by the coda waves. Deeper sources do not excite surface waves as easily as do shallow sources. Therefore, the codas for the deep data set will be largely composed of body waves. Sato (1977) showed that the geometrical spreading term in the power spectrum is approximately equal to t^{-2} when the coda is composed entirely of singly backscattered body waves (see equation 3.4). Thus, equation 3.5 will hold for all of the data used in this thesis.

CHAPTER IV

CALCULATING CODA-Q

The method used to calculate coda-Q in this thesis is the same as that used by Aki and Chouet (1975) with slight modifications by Kvamme (1985). The basic task is to fit equation 3.5 to the envelope of band pass filtered coda waves. Taking the log of 3.5 simplifies the fitting process. The new form is

$$ln\,(A\,(f\ ,\ t)\ t^{u}) = ln\,(C(\ f\ )) - \pi f\,t\,/Q \qquad (4.1)$$

In a narrow frequency band, the coda source factor $C(f\ )$ is assumed to be constant and accounts for the effects of the earthquake source, the station site, and backscattering (Phillips et al., 1986). Furthermore, in practice, all other time independent parameters, such as the instrument response, will be included in the $C(f\ )$ term (Kvamme, 1985). Equation 4.1 is the equation of a straight line of slope $-\pi f\ /Q$ and Q is calculated from the slope of the line which best fits the amplitude values in the least squares sense. Thus, a Q value is obtained for the particular value of the center frequency of the band used to filter the seismogram. It is assumed that u is a constant and that Q is constant in a narrow frequency band. Note that the value of Q that is obtained is dependent on the choice of the value u .

Repeating the above fitting procedure for many bandpass filtered seismograms and averaging the results yields an estimate of Q at the center frequency of the band. Repeating the entire process for different bands yields an estimate of Q as a function of frequency, $Q(f\ )$.

Several difficulties are encountered when using the coda-Q method. See Kvamme (1985) for a more detailed discussion of these difficulties. The problems are related to calculating the amplitude envelope of the coda, the quality of the least squares fit of equation 4.1 to this envelope, bandpass filtering the seismogram, noise, the choice of u in equation 4.1, origin time error, and the choice of the time window used in the analysis.

Coda Envelope. Fitting equation 4.1 to the filtered coda envelope can be difficult in practice because of temporal fluctuations in the peak amplitudes of the coda. The difficulty arises in trying to create an algorithm which is not adversely affected by the temporal fluctuations (Kvamme, 1985). Equation 3.5 applies to the envelope as drawn through the peak values of the seismic trace. An alternative type of envelope which is very nearly parallel to the envelope of the peak values is the root-mean-square (rms) envelope. It is not seriously affected by temporal fluctuations in the coda amplitude. This envelope is calculated by averaging amplitudes over a time window 5 cycles-long. The algorithm is given by,

$$a_k = \sqrt{\frac{1}{2c} \sum_{i=k-c}^{k+c} S_i^{\,2}}$$

where a_k is one point on the envelope function $A(f,t)$, $c = 5/(2f\,\Delta t)$, Δt is the digital data sampling interval, and S_i is the amplitude of the seismic trace. Kvamme (1985) showed that coda-Q values calculated from the rms envelope differ from the values calculated using the envelope of the peak values by less than 10%. I used the rms envelope for all of the coda-Q calculations in this thesis. An example is illustrated in figure 4.1.

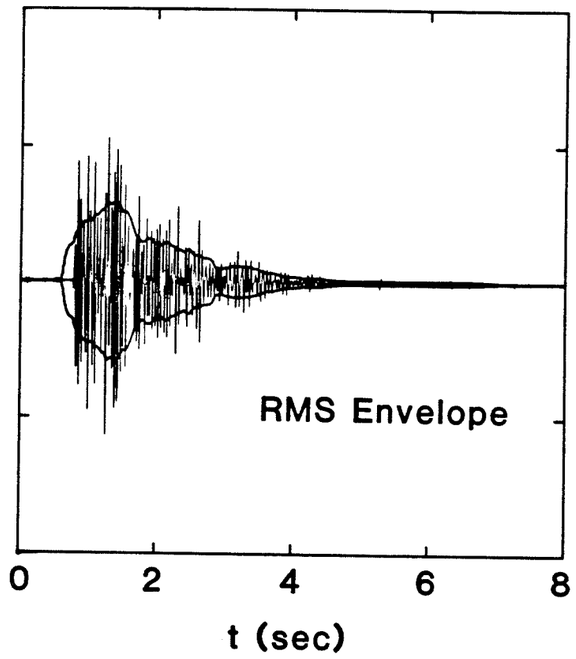

Figure 4.1 The root-mean-square amplitude envelope. The seismogram (velocity vs. time) is from the shallow data set at Mt. St. Helens and was bandpass filtered at 12.0 ± 4.0 Hz.

Least Squares Fit. The reliability of each Q value that is calculated for each bandpass filtered trace depends on the quality of the least squares fit of equation 4.1 to the rms envelope. The parameter which is used to measure the fit is the correlation coefficient (ρ) (Bevington, 1969). The value of ρ ranges from 0 to 1.0 with 1.0 representing a perfect fit, that is, when all of the points lie exactly on the best fit line. By setting strict minimum values for ρ we have some control over the reliability of the Q results. This minimum value of ρ is somewhat arbitrary, but it represents a trade-off between the standard error of the mean-Q and the number of Q values to be averaged at each frequency. When the minimum value was set below 0.45 the resulting average Q values had unacceptably large standard errors. When it was set higher than 0.45, only a few of the "fits" met the requirement of the minimum ρ, and the number of Q values to be averaged was unacceptably small. Throughout the coda-Q analysis, the minimum value of ρ was set at 0.45.

Bandpass Filtering. In order to use equation 3.5 we must bandpass filter the seismograms into narrow frequency bands. The filters used are eight-pole recursive Butterworth filters with zero phase lag. Kvamme (1985) showed that using these filters to calculate coda-Q from synthetic data reproduces the correct Q values, indicating that they are satisfactory for use with real data.

An important filter effect which was encountered during the course of this thesis research is caused by the use of relatively short coda windows and the sharp truncation of the trace at the beginning of the coda sample which produces a ringing amplitude response by the filter that may take several cycles to decay to negligible amplitude. At lower frequencies the short windows used in this thesis may be comparable in length to the time it takes for

the ringing to decay. Thus, the amplitude would be in error due to the ringing of the filter. This effect was avoided by first filtering the entire seismogram and then sampling the coda so that the truncation takes place after filtering.

Noise. In the theoretical development of equation 3.4 the assumption was implicitly made that there is no noise in the seismic signals being analyzed. Noise affects the later parts of the coda where the amplitude has decayed to the extent that the amplitude of the noise is comparable to the coda amplitude. Using synthetic data Kvamme (1985) showed that the Q values calculated from data with noise will tend to increase as the lapse time increases. Furthermore, the calculated value of Q increases as the noise level increases. This is to be expected since the presence of noise causes the trace amplitude to decay more slowly than the true coda amplitude. The result is that the slope of the best fit to the rms amplitude will be smaller, leading to an overestimation of Q (see equation 4.1). To minimize the effect of noise on the calculated coda-Q values, the minimum value for the signal to noise ratio was set at 5.0 for all of the analysis at MSH. The signal to noise ratio is calculated by taking the ratio of the signal level at the end of the coda sample to the level of the noise prior to the first arrival of the seismogram. The choice of 5.0 for the minimum signal to noise ratio allowed long enough coda windows to give reasonably small standard errors for the Q values (see below), while ensuring that noise did not cause a serious overestimation of the Q values (see Kvamme, 1985).

Spreading Parameter. When the least squares fit of equation 4.1 is performed the envelope values must be corrected for geometrical spreading. This correction has the form t^{-u} where t is the lapse time and u is the spreading parameter. There is some uncertainty about the appropriate value

of u since u depends on the types of waves composing the coda and the degree of scattering occurring in the medium. In some studies, u is treated as a free variable (eg. Aki and Chouet, 1975). From equation 4.1, Q should increase with increasing u. However, Kvamme (1985) and Aki and Chouet (1975) showed that u has only a slight effect on the Q values which are calculated when u is between 0.5 and 1.0. For most frequencies, the calculated Q values vary by less than 20% as u varies from 0.5 to 1.0 (Rautian and Khalturin, 1978).

Aki (1980) showed that in the lithosphere the calculated values of coda-Q agree closely with the direct shear wave Q calculated by the spectral ratio method. I have assumed throughout the coda-Q calculations for this thesis that the coda is composed of singly backscattered shear waves and therefore u was set at 1.0. The coda is probably composed of a mixture of wave types that have been subjected to varying degrees of scattering. In addition, the composition of the coda is likely to be dependent on frequency. Thus, the correct choice for u may be less than 1.0. However, in Chapter VII, it will be shown that coda-Q results at MSH will hold for all values of u between 0.5 and 1.0, and that 1.0 is the most conservative value that can be chosen.

Origin Time Error. Any error in the origin time will cause an error in the correction for geometrical spreading and hence error in the calculated value of Q (see equation 3.4). Assuming that the calculated value of the origin time is in error by amount Δt then equation 4.1 can be written,

$$ln\,(A\,(f\ ,\,t\,)) + u\ \ ln\,(t+\Delta t\,) = ln\,(C\,(f\ )) - \frac{\pi f}{Q}(t+\Delta t\,)$$

where t is the correct time since earthquake origin. Figure 4.2 illustrates the effect of origin time error on the calculated value of Q for different

values of Δt and a correct Q value of 100. Note that when $\Delta t < 0$, the calculated Q is too large, and when $\Delta t > 0$, Q is too small. Also note that the error in the calculated Q values are largest for short lapse times. At MSH Δt is of the order 0.1 second and the earliest lapse time in any of the coda windows used is 2.0 seconds. Figure 4.3 illustrates the effect of this origin time error on the calculated Q values. Note that Q will be in error by about 5 to 10 percent for Q in the range 10 to 100 which is approximately the range observed at MSH.

It can be assumed that any errors in the origin time are arrival-time picking errors and are thus (approximately) random errors so that the errors in the origin times will have a zero mean. Random errors will cause an increase in the scatter of the Q values but will not affect the average value.

The Coda Window. There are two important criteria for the selection of the coda window. The first is the window start criterion. Rautian and Khalturin (1978) found that the seismograms of small local tectonic earthquakes consist primarily of coda waves for lapse times greater than twice the S-wave travel time (t_s) and consist entirely of coda waves after $3t_s$. Therefore the window start criterion requires that the coda window be started later than twice the S-wave travel time. The second criterion is the signal to noise criterion which requires that the signal to noise ratio (s/n) be greater than 5.0 so that the effect of noise on the coda-Q values is minimized.

The choice of window length has a direct effect on the standard errors of the average Q values. Within the coda there are fluctuations in the values of the rms amplitude with time. The shorter the coda window the more likely it is that these variations in amplitude will seriously affect the slope of the coda decay and hence the calculated Q. The average Q calculated using very short windows will have large standard errors. As the window is made

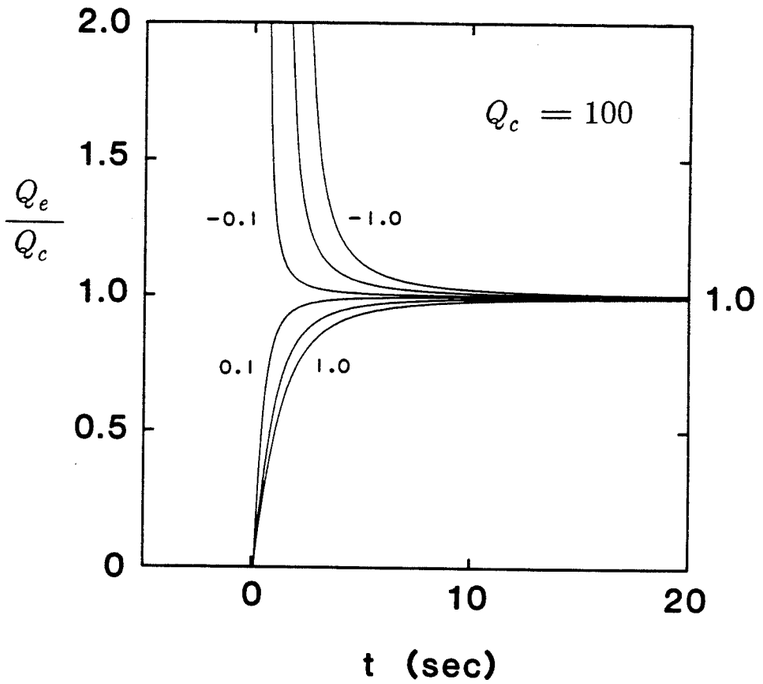

Figure 4.2 Origin time error and the calculated Q value #1. The ratio of the erroneous Q value, Q_e, to the correct Q value, Q_c, is plotted as a function of lapse time. Each curve corresponds to a different error in the origin time, as indicated, with the upper (lower) intermediate curve corresponding to an error of – 0.5 (+ 0.5) sec.

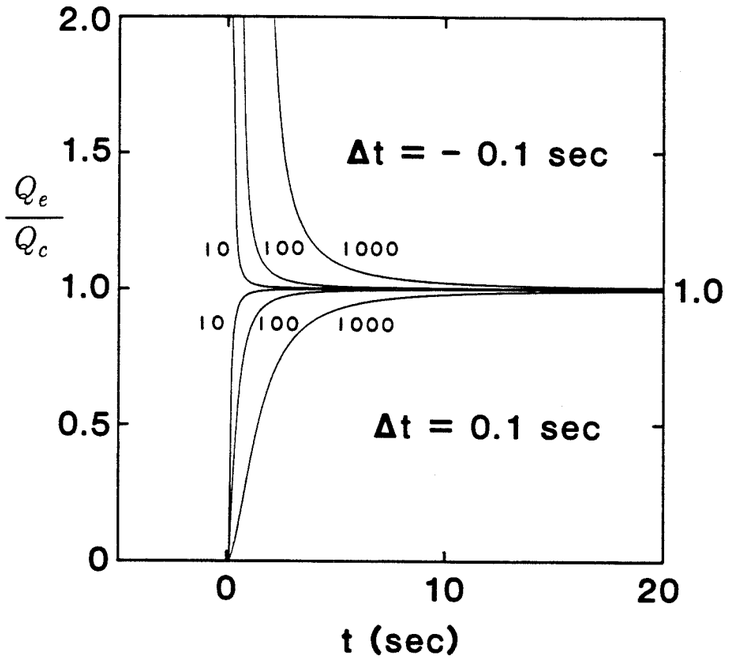

Figure 4.3 Origin time error and the calculated Q value #2. The ratio of the erroneous Q value, Q_e, to the correct Q value, Q_c, is plotted as a function of lapse time. Each curve corresponds to a different value of Q_c as indicated. Upper (lower) curves were calculated using $\Delta t = -0.1$ ($\Delta t = +0.1$).

longer the fluctuations will tend to average out over the length of the window resulting in reduced standard errors. Therefore it is desirable to have the coda window long enough to minimize the effect of these fluctuations in the coda amplitude, while still satisfying the window start and signal to noise criteria. For the coda-Q calculations on the MSH data, a window of length 5.0 seconds was used, except when the values of the Q-structure model were calculated (see chapter VII). The five second window was the longest one that would satisfy the above criteria for the data used and is shorter than the windows used in most coda-Q studies. This is because of the relatively short duration of the seismograms in the data used for this thesis (10 to 15 seconds) compared to the data used in most other studies. In principle, one could use larger events which would have longer codas, but the limited dynamic range of the recording system at the University of Washington tends to "clip" the peak amplitudes of seismograms of larger events causing a large fraction of a given seismogram to be useless for coda-Q calculations. The five second window proved to be satisfactory for the MSH data used for this thesis because it produced Q values with acceptable standard errors.

Procedure Used to Calculate Coda-Q

The procedure used to calculate coda-Q takes into account all of the above considerations. First a list of candidate events is compiled from the catalog of events based on suitable locations and focal depths. Second, the seismic traces are inspected by eye to ensure that all data that are used have satisfactory signal to noise ratio, that the trace amplitudes in the coda are not clipped, and that each seismogram records only one earthquake. Next the data are loaded onto a computer for analysis. A computer program

developed by Jens Havskov, from the University of Bergen, analyzes each seismic trace separately. The entire trace is bandpass filtered into a narrow band of specified center frequency and bandwidth (see chapter VI). Filtering before windowing avoids the effect of the filter ringing due to the sharp truncation of the coda window. Next, a sample of the coda is taken (windowed) at the specified window start time. The window start time is checked to ensure that it satisfies the window start criterion. If it fails this test, the filtered trace is rejected from the analysis. Next the signal to noise ratio is calculated and if it is less than 5.0 then the trace is rejected. Assuming it passes this test, the rms envelope is calculated. Next equation 4.1 is fit to the rms envelope after it has been corrected for geometrical spreading and a value of Q is determined at the center frequency of the band. The fit is by least squares (linear regression) and is illustrated in figure 4.4. The quality of the fit is measured by the correlation coefficient (ρ). A test is performed at this point to ensure that $\rho \geq 0.45$. If $\rho < 0.45$ then the corresponding Q value is rejected from the analysis. Assuming that ρ is satisfactory then the Q value is stored and the next seismic trace is analyzed in the same way.

Repeating the above process for many seismograms and averaging the results leads to an estimate of the mean value of Q at the center frequency of the band. The uncertainty of the estimate of the mean is calculated as a standard error of the mean (σ) using the following algorithm,

$$\sigma(f) = \sqrt{\frac{1}{N(N-1)} \sum_{i=1}^{N} (Q_i(f) - Q_a(f))^2}$$

where Q_a is the average Q at the frequency f. Repeating the entire process for different center frequencies yields an estimate of $Q(f)$ for the volume of the earth that the coda waves have been sampling.

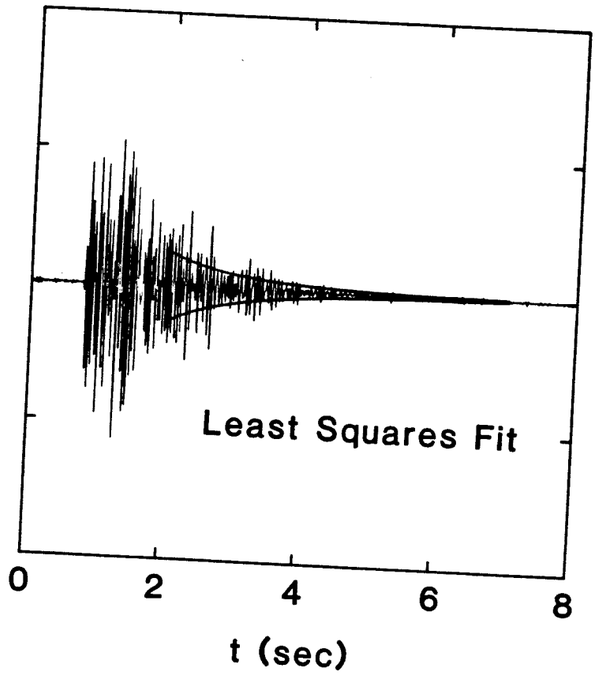

Figure 4.4 Least Squares fit to the rms envelope. The seismogram (velocity vs. time) was bandpass filtered at 12.0 ± 4.0 Hz.

CHAPTER V

SIMPLE Q-STRUCTURE MODEL

Coda-Q measures the properties of the rocks through which the coda waves have traveled. These rocks are located in a volume of the earth's interior surrounding the earthquake source and the receiver. The size of this volume depends on the time since the earthquake origin. Sampling the coda at different times corresponds to sampling different sized volumes of rock. Thus, by calculating coda-Q at different window times one can calculate coda-Q within different sized sampling volumes and thereby determine the "Q-structure" in the earths interior. This approach was used at MSH to derive a Q-Structure model.

Sampling Volume. Coda-Q is a measure of the average properties within the volume of rock which has been sampled by coda waves. The actual size and shape of the sampling volume depends on the details of the velocity structure near the source and receiver, and the degree of scattering occurring in the medium. At MSH the velocity structure in the shallow crust is complex and not well known. The degree of scattering can be estimated by taking the spectral ratio of shear waves to coda waves (Herraiz and Espinosa, 1986; Aki and Chouet, 1975). However, at MSH there are few calibrated stations and few earthquakes with clear S phases so I made no attempt to determine the degree of scattering. Therefore, it is difficult to specify the shape and size of the sampling volumes at MSH. In general one would expect that the shape will be rather irregular due to the complex velocity structure. Although the actual volume cannot be specified, it can be

represented by assuming single scattering and a uniform velocity structure (independent of position). In that case it will take on the shape of an ellipsoid with the source and receiver at the foci (see figure 5.1). The size of this sampling volume is calculated by taking the time at the center of the coda window t_v. The sampling ellipsoid has semi-major axis $a_1 = v\ t_v/2$ where v is the shear wave velocity and semi minor axis $a_2 = \sqrt{a_1^2 - D^2/4}$ where D is the distance between the source and receiver (Pulli, 1984). At MSH a reasonable average shear wave velocity in the crust to depths of 10 km or so is 3.0 km/sec and this value was used to calculate a_1. Note that later windows correspond to larger sampling volumes since a_1 is proportional to t_v.

Model for the Spatial Variation of Q. The Coda-Q results which are presented in chapter VII indicate that the volcano is more highly attenuating (lower Q) than the medium surrounding it. This indicates that there is a spatial variation of Q at MSH. In this section a simple mathematical model is derived for this variation. The goal of determining such a model is to use it to attempt to separate the effects of the seismic source from the effects of the medium on the seismograms of volcanic earthquakes. In chapter VIII the results of the attempted separation of these effects are discussed. A simple model which is consistent with the coda-Q results consists of a small volume of crust at the volcano with lower Q than the surrounding medium. Since it is assumed that the coda is composed of backscattered shear waves, which are spherical waves, then the simplest model will have spherical symmetry. One such model is illustrated in figure 5.2 and consists of a small hemispherical volume at MSH with attenuation described by $Q_1(f)$, surrounded by a medium with attenuation described by $Q_2(f)$. The center of the volcano corresponds to the point $r = 0$.

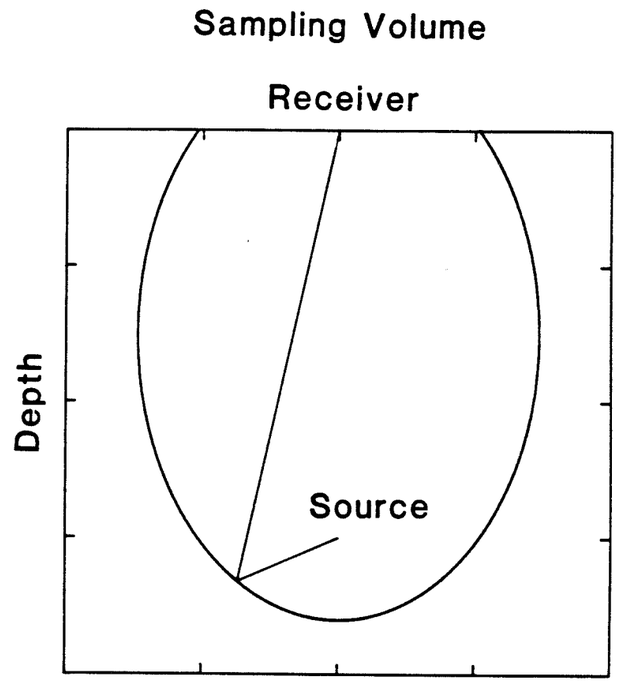

Figure 5.1 Vertical Cross-Section of the Sampling Volume. Assuming single backscattering of shear waves the sampling volume is an ellipsoid with the source and receiver at the foci.

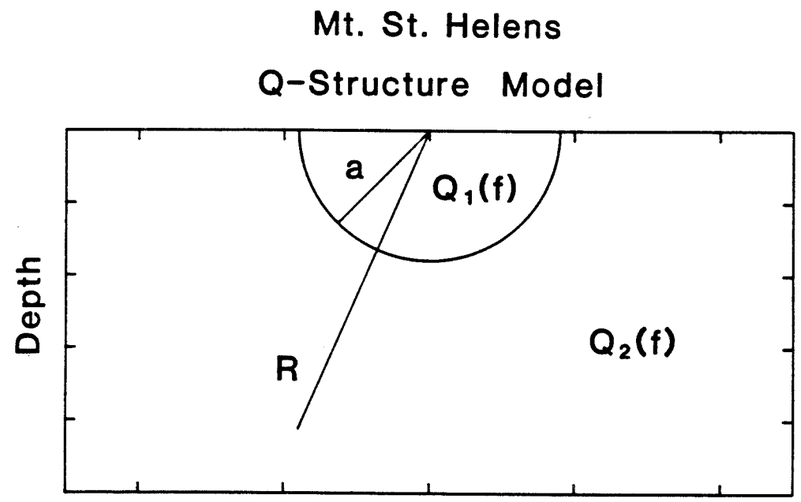

Figure 5.2 The Q-structure model. Shown above is a vertical cross-section of the model which consists of a a hemisphere of radius a with attenuation described by $Q_1(f)$ surrounded by a medium with attenuation described by $Q_2(f)$. R specifies the location of a scatterer. The center of the volcano corresponds to the point $R = 0$.

In the following derivation I assume that the source and receiver are in the same location, that the shear wave velocity is independent of position, and that single scattering is the type of scattering occurring throughout the medium. Consider a spherical wave which is emitted by the source at $r = 0$. As it expands from the source it is attenuated by the factor $e^{-\pi f t_1/Q_1}$ until it has traveled a distance a, where t_1 is the time spent in the volume $r < a$. For $r > a$ the wave will be attenuated by the factor $e^{-\pi f t_2/Q_2}$ where t_2 is the time spent in the region $r > a$. At some radius R the wave is scattered back toward the source and receiver and the reverse sequence of attenuation will occur for the scattered wave. Equating the total attenuation with the cumulative attenuation experienced by the wave in the different regions of the model yields,

$$e^{-\pi f t/Q} = e^{-2\pi f t_1/Q_1} e^{-2\pi f t_2/Q_2}$$

where Q is the total attenuation and t is the lapse time. Now, $t_1 = a/v$, $t_2 = (R-a)/v$, and $t = 2R/v$ where v is the wave velocity. Taking the logarithm of both sides of the above equation, substituting for t, t_1, and t_2, and simplifying yields

$$\frac{1}{Q(f,R)} = \frac{a}{R}\frac{1}{Q_1(f)} + \frac{(R-a)}{R}\frac{1}{Q_2(f)} \qquad (R>a) \quad (5.1)$$

This equation is a weighted average of the contributions of Q_1 and Q_2 to the total Q. The weighting is determined by R and a. Note that $R = v\,t/2$ so that R is proportional to time, and thus, the condition that $R > a$ is equivalent to the condition $t > 2\,a/v$. Figure 5.3 illustrates this model equation assuming different values of R/a and hypothetical functions

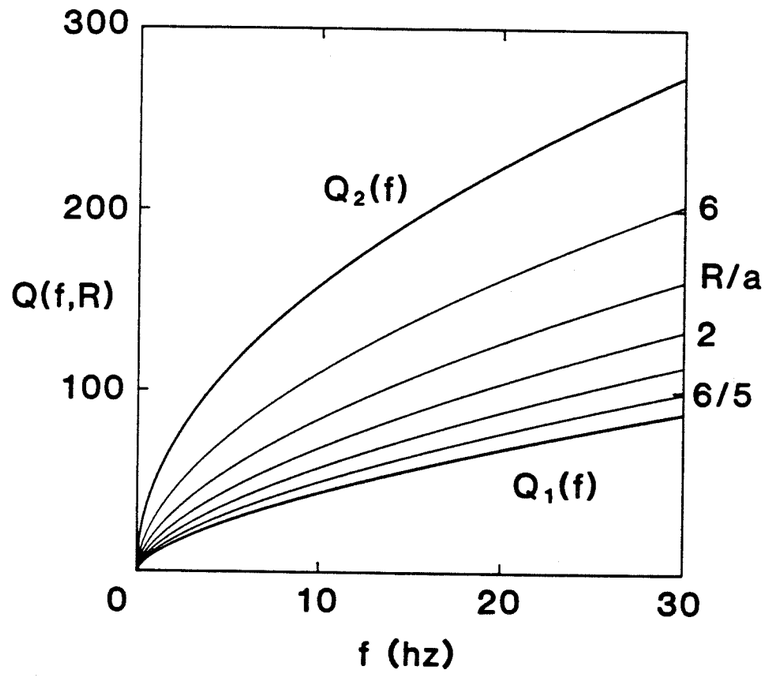

Figure 5.3 Plot of equation 5.1. $Q(f,R)$ is a weighted average of $Q_1(f)$ and $Q_2(f)$. The top and bottom curves are Q_2 and Q_1 respectively. Intermediate curves are plots of $Q(f,R)$ corresponding to different values of R/a. From the top $R/a = 6, 3, 2, 2/3$, and $6/5$.

$Q_1(f)$ and $Q_2(f)$ with $Q_1 < Q_2$. Note that $Q(f, R)$ is intermediate between Q_1 and Q_2. I used equation 5.1 to calculate Q_1 and Q_2 at MSH by forward modeling. The details of this calculation are discussed in chapter VII.

CHAPTER VI

DATA

Seismograms of earthquakes located at MSH from 1982 to 1986 were used in the coda-Q analysis. The earthquakes were located directly beneath or within the volcanic structure (see figure 6.1). All of the seismograms used are of the impulsive medium-frequency and high-frequency types, and were digitally recorded from telemetered short-period vertical instruments located on the flanks, in the crater, and on the dacite dome of MSH. Digitization was done at a rate of 100 samples per second. Only well located events were used with uncertainties of roughly 1 km in depth and 0.1 second in origin time. The earthquakes range in magnitude from 0.5 to 1.5 on the duration magnitude scale developed by (Crosson, 1972). Although thousands of earthquakes have been recorded at MSH only a small fraction are suitable for coda-Q analysis. While there are many impulsive medium and high frequency earthquakes, only a small fraction of these have both a large signal to noise ratio and are not "clipped" by the limited dynamic range of the recording system. The duration of these events ranges from roughly 10 to 20 seconds. The data were divided into two sets based on hypocentral depth (see figure 6.2).

Shallow Data Set. The shallow data set consists of 30 seismograms from 24 earthquakes located at depths of 0 to 2 km. The shallowest of these are probably originating in the dome while the deepest of these are located in a small volume beneath the dacite dome in the crater. Most of the hypocenters are shallower than 1 km so they are most likely located within the volcanic structure. An example of a seismogram from the shallow data set is

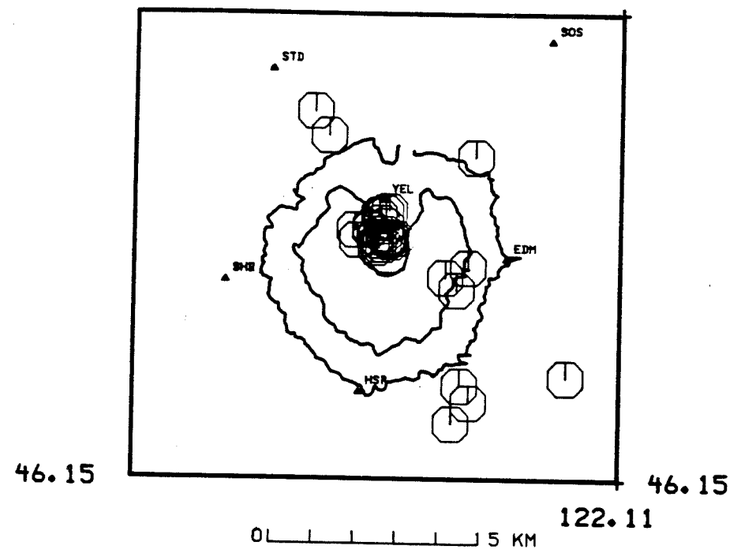

Figure 6.1 Epicenters of earthquakes. Octagons are epicenters and triangles are telemetered seismic stations. Label for dome station NSP is covered by epicenter symbols.

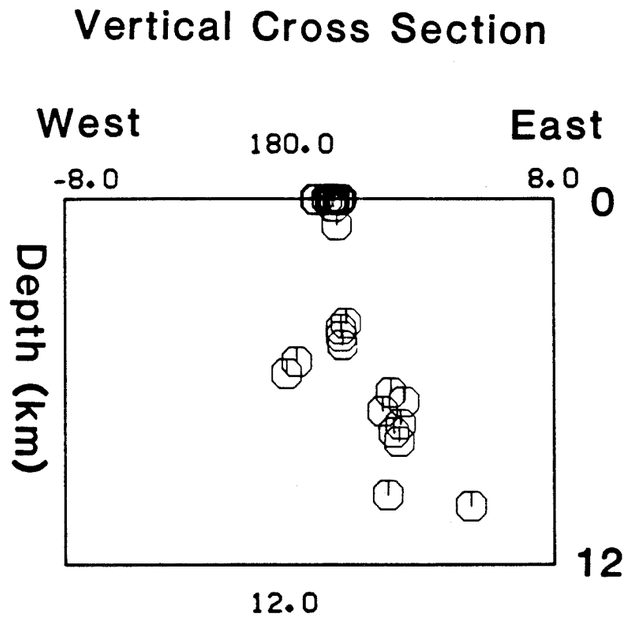

Figure 6.2 Hypocenters of earthquakes. The vertical E-W cross section shows the hypocenters (octagons) of the shallow data set (0 to 2km) and the deep data set (4 to 10 km).

shown in figure 4.1. The shallow data set was recorded on only two stations. The dome station was called NSP and the crater station is called YEL (see figure 6.3). The focal distances to these stations are less than about 2.0 km (see figures 6.1 and 6.2) which is smaller than the distance traveled by most of the coda waves in the sampled windows which ranges from 3 to 17 km. This means that the sampling volumes are roughly spherical in shape. Also, the assumption of zero source-receiver distance, which is implicit in the use of equation 3.5, holds better for the shallow data set than for the deep data set.

A significant fraction of the waves composing the codas of the seismograms in the shallow data set are likely to be surface waves. The volcano is composed of rocks with low seismic velocities compared to the surrounding crust and the incident angles will be large (grazing) for a large fraction of the surfacing body waves (direct or scattered), which will result in surface waves. The presence of surface waves in the coda will tend to cause the calculated Q values to be in error because the spreading parameter u is assumed to be 1.0 which is appropriate for body waves. If our chosen value for u is too large then the calculated value of Q will be too large (see equation 3.5). In addition, the assumption of single scattering may be incorrect. If the waves composing the coda have been multiply scattered then the calculated values of Q will be too large. However, (Gao et al., 1983) showed that the effect of multiple scattering should cause an overestimation of Q by a factor of less than 1.4.

Deep Data Set. The deep data set consists of of 17 seismograms from 14 earthquakes located at depths of 4 to 10 km. These events are of the high-frequency type and their seismograms are indistinguishable from normal tectonic seismograms when recorded on stations located away from the volcano. The foci for these events are probably located below the volcanic

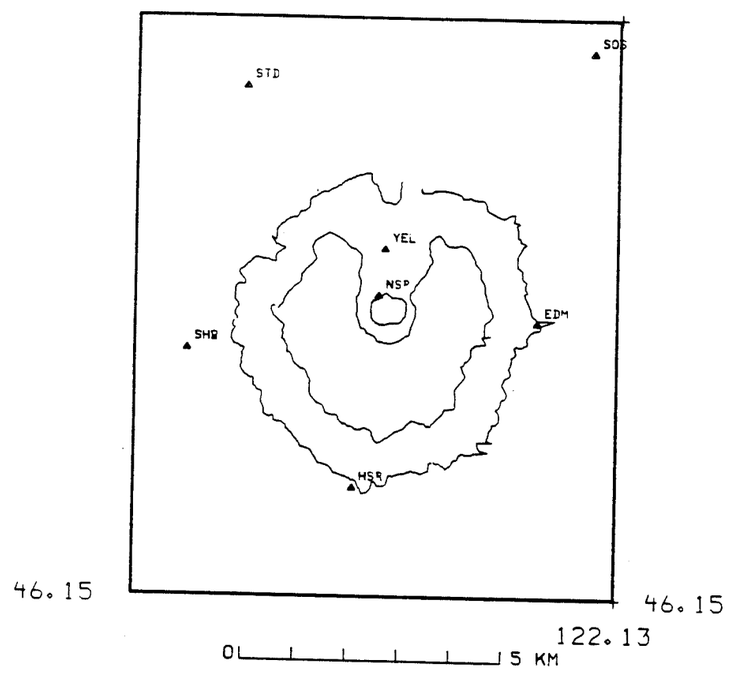

Figure 6.3 Map showing seismic stations at Mt. St. Helens. All stations are equipped with telemetered short-period vertical seismometers. Note the station on the dome NSP.

structure. The deep data set was recorded on only one station, YEL, which is located in the crater. The coda of a seismogram from the deep data set is less likely to contain as much surface wave energy as the coda of a seismogram in the shallow data set because body waves which surface near the epicenter will have smaller incident angles. The separation between the sources and receivers for the deep data set ranges from about 7 to 12 km which is comparable to the distance traveled by the coda waves for these deep events which ranges from about 7 to 17 km. This means that the geometrical spreading term in equation 3.5 should be replaced by Sato's term (see equation 3.3). However, since all of the coda samples satisfy the window start criterion, the spreading term in 3.5 will be approximately equal to Sato's term (see equation 3.4).

Frequencies and Bandwidths. The convention in coda-Q calculations is to use octave center frequencies and log-unit bands so that when plotted on a log scale the coda-Q points will be evenly spaced. The center frequencies and bands established by Aki are the ones most often used and they are shown in table 6.1. Note that the bands do not overlap so that the calculated Q values are independent. These values were used to calculate some of the coda-Q values for this thesis. Another set of frequencies and bands that were used is shown in table 6.2, and these also do not overlap. When calculating values of the Q-structure model it is desirable to use smaller bands so that Q is determined at a larger number of frequencies. In so doing, the model can be specified without relying too much on interpolation (see chapter VIII). The frequencies and bands used to calculate the model are shown in table 6.3. Note that the bands slightly overlap so that the values of the model are not entirely independent. Thus, some "smoothing" of the model values has occurred.

Table 6.1 Frequencies and bandwidths #1. These values were originated by Aki.

Frequencies and Bands	
f (Hz)	Δf
1.5	1.0
3.0	2.0
6.0	4.0
12.0	8.0
24.0	16.0

Table 6.2 Frequencies and bandwidths #2. These values were used to calculate coda-Q from some of the MSH data.

Frequencies and Bands	
f (Hz)	Δf
2.0	5.0
7.0	5.0
12.0	5.0
17.0	5.0
22.0	5.0
27.0	5.0
32.0	5.0

Table 6.3 Frequencies and bandwidths #3. These values were used to calculate values of the Q-structure model at MSH.

Frequencies and Bands	
f (Hz)	Δf
2.0	1.5
6.0	4.5
10.0	8.0
14.0	10.5
18.0	14.0
22.0	17.0
26.0	19.5

CHAPTER VII

RESULTS AND DISCUSSION

There are 2 important results from the coda-Q analysis at MSH. First, the coda-Q values corresponding to a small shallow volume of rock near (and including) the volcano are much lower than the coda-Q values corresponding to a much larger volume of rock surrounding the volcano. Second, the coda-Q values corresponding to a shallow volume of rock near (and including) the volcano are slightly lower than the values corresponding to a slightly deeper volume of rock near (and including) the volcano. These two results indicate that Q is lower at MSH than it is in the surrounding crust. A simple model for this Q-structure was derived in chapter V. The values of the model are discussed below.

Coda-Q Result 1. Coda-Q values were calculated at MSH using the earliest possible window start time, so that the smallest sampling volume could be used. The shallow data set allowed earlier start times than the deep data set due to the shorter S-wave travel time to stations in the crater. Recall that when calculating coda-Q the coda window must be started after twice the S-wave travel time (see chapter IV). The sampling volume for this earliest window is a hemisphere about 6 km in radius, centered on the dome. The aim of using the smallest volume was to measure, to the greatest extent possible, the properties of the volcano alone. The coda-Q results for this volume of rock are shown in table 7.1 and figure 7.1. The values range from about 10 at 1.5 Hz to 100 at 24 Hz.

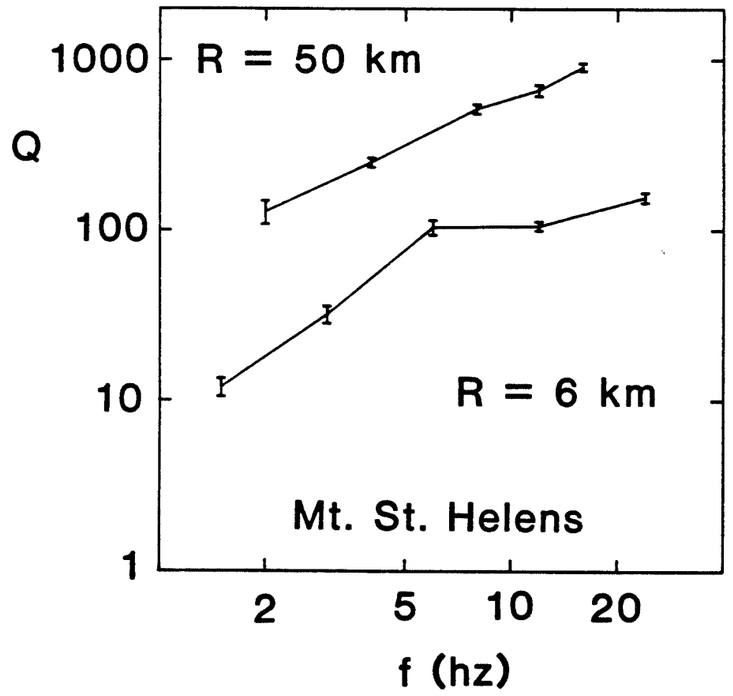

Figure 7.1 Coda-Q result #1. Coda-Q for Mt. St Helens is compared to coda-Q for the surrounding crust and upper mantle. Error bars are one standard error of the mean. f is frequency in Hertz. Lower curve is calculated from the shallow data set and corresponds to a sampling volume 6 km in radius. Upper curve was calculated by Havskov et al. (1987) and corresponds to a volume roughly 50 km in radius.

Table 7.1 Coda-Q from the shallow data set (2 sec). N is the number of bandpass filtered seismograms used to calculate the average Q at each f (Hz), and σ is the standard error of the mean.

MSH Shallow Data Set			
f	Q	σ	N
1.5	12	1.5	17
3.0	32	3.7	14
6.0	104	10.4	17
12.0	106	6.4	28
24.0	156	10.6	24

Table 7.2 Coda-Q values calculated by Havskov et al. (1987). N is the number of bandpass filtered seismograms used to calculate the average Q at each f (Hz), and σ is the standard error of the mean.

Havskov etal (1987)			
f	Q	σ	N
2	128	19.9	10
4	249	15.4	20
8	516	33.7	18
12	666	49.8	16
16	910	47.8	16

Coda-Q values for the crust surrounding MSH were calculated by Havskov et al. (1987). The data used to calculate these values are seismograms of tectonic earthquakes which were recorded on stations located in the region surrounding the volcano. The epicenters of these earthquakes were located 17 km north of the volcano, near Elk Lake. The sampling volume corresponding to the Havskov values is nearly hemispherical and about 54 km in radius and centered roughly 10 km north of the volcano. The coda-Q values are shown in table 7.2 and figure 7.1, and range from about 100 at 2 Hz to 1000 at 16 Hz. Recall that coda-Q measures the spatial average of $Q(f)$ within the sampling volume. Thus, these coda-Q results indicate that the average $Q(f)$ is about an order of magnitude lower at MSH, and the shallow crust beneath it, than the average $Q(f)$ in a large volume of crust (and possibly upper mantle) surrounding the volcano.

It is likely that the codas are composed of some mixture of surface and body waves and that some degree of multiple scattering has occurred. The presence of surface waves in the coda will cause the coda-Q values to be overestimated when singly backscattering body waves are assumed in the calculations. However, this overestimation is expected to amount to no more than 20%. If multiple scattering occurs to a significant degree, then Q will also be overestimated, but at most by a factor of 1.4. Thus, the maximum possible effect of these sources of error in the Q values is a factor of $(1.4)(1.2) = 1.68$. Assuming that only the Havskov values are affected then we might expect the correct values to be a factor of $1/1.68$ smaller. Therefore, the Havskov values would still be at least a factor of 5 larger than the values for the shallow data set at MSH. Thus, even allowing for the maximum possible expected error in the Q values, the results in figure 7.1 indicate that the spatially averaged Q-structure is significant at MSH.

Coda-Q Result 2. Two comparisons are made between the coda-Q values for the shallow data set and the values for the deep data set. The first comparison is made by using a window start time of 4.5 seconds for both the shallow and deep coda-Q calculations. This start time is the earliest time for which coda-Q values can be calculated for the deep data set because most of the deeper seismograms have S-wave travel times which exceed 2 seconds, and the coda window must be started later than twice the S-wave travel time. The coda-Q values for the two data sets are very similar at this window start time with the values for the shallow data set slightly lower for all but the highest frequency (see tables 7.3 and 7.4 and figure 7.2). (Note that the two Q values have overlapping standard errors at this highest frequency). The similarity between the curves is to be expected since the corresponding sampling volumes are also very similar (see figure 7.3). The volume for the shallow data set is very nearly hemispherical due to the small distances between the sources and receivers for these shallow events. The radius for this volume is about 10 km. The volume for the deep data set is slightly ellipsoidal due to the greater depth of the sources and thus samples more of the deeper crust beneath the volcano. The semi-major axis for this ellipsoid is roughly 13 km in length. This comparison indicates that, at MSH, the average $Q(f)$ in the shallow crust is slightly lower than the average $Q(f)$ in the shallow and slightly deeper crust. The codas in the shallow data set are likely to be composed of surface waves to a greater degree than the codas in the deep data set because the shallow sources, located in lower velocity materials, can more easily excite surface waves at stations near the epicenter. Therefore, the coda-Q values for the shallow data set are likely to be overestimated by as much as 20%. Thus, the actual values for the shallow curve in figure 7.2 are likely to be smaller than those shown, so that the difference between the shallow and deep curves is probably greater. Thus,

Table 7.3 Coda-Q from the shallow data (4.5 sec). N is the number of bandpass filtered seismograms used to calculate the average Q at each f (Hz), and σ is the standard error of the mean.

Shallow Data Set 4.5 sec			
f	Q	σ	N
2	45	6.9	13
7	74	5.9	21
12	83	5.4	20
17	105	8.3	19
22	224	28.1	15

Table 7.4 Coda-Q from the deep data set (4.5 sec). N is the number of bandpass filtered seismograms used to calculate the average Q at each f (Hz), and σ is the standard error of the mean.

Deep Data Set 4.5 sec			
f	Q	σ	N
2	84	26.6	3
7	112	6.4	3
12	127	16.0	4
17	137	27.1	3
22	188	42.4	2
32	529	15.6	2

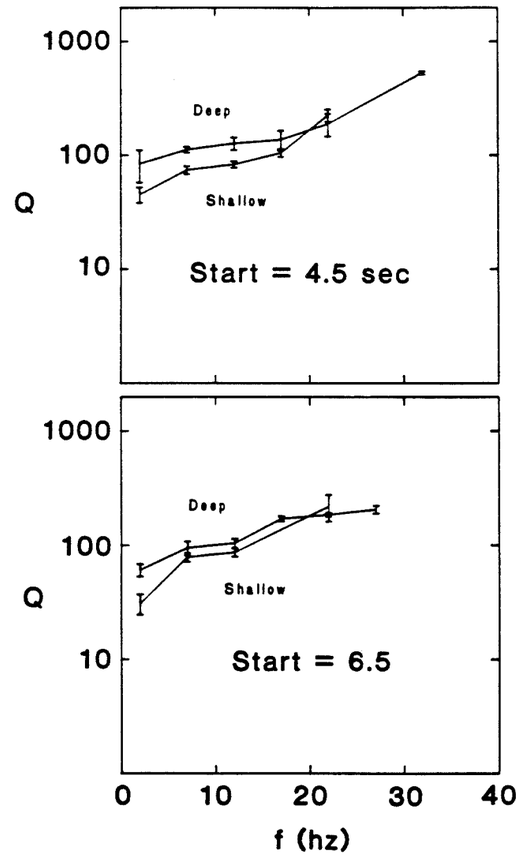

Figure 7.2 Coda-Q result #2. Coda-Q for the shallow data set is compared to coda-Q for the deep data set at two different window start times. Error bars are one standard error of the mean. f is frequency in Hertz. Upper (lower) frame shows values calculated using a window start time of 4.5 (6.5) sec. Upper (lower) curve in each frame is from the deep (shallow) data set.

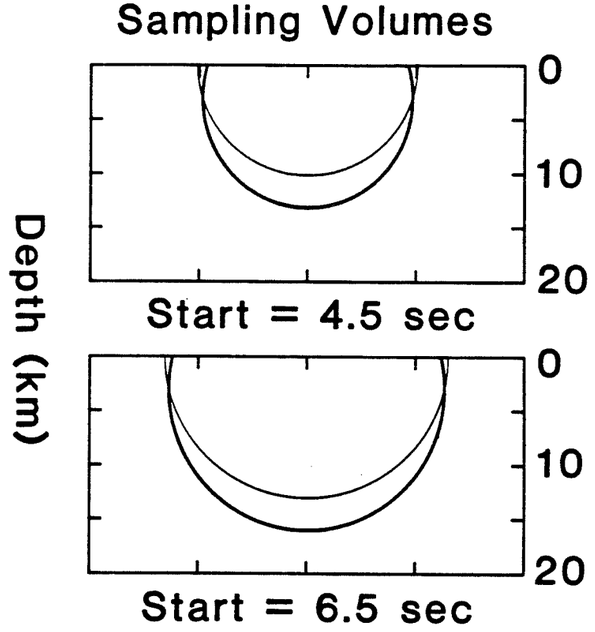

Figure 7.3 Sampling volumes for coda-Q result #2. Sampling volumes for the shallow and deep data sets are compared at two different window start times. Curves show vertical cross sections of the sampling volumes. Upper (lower) frame shows the volumes for the start time of 4.5 (6.5) sec. Heavier (lighter) curve in each frame is from the deep (shallow) data set.

the assumption that the codas of all of the data are composed of singly back-scattered body waves is a conservative one, since if it fails, the difference shown in figure 7.2 will be increased.

The second comparison was made by using a window start time of 6.5 seconds for the coda-Q values from both data sets. This start time is the latest one for which coda-Q values can be calculated from the shallow data set because of the short duration of the seismograms from the shallow data set. The signal to noise ratio becomes too low (< 5.0) when start times later than 6.5 seconds are used. The coda-Q values for the two data sets are more similar at the start time of 6.5 seconds than at 4.5 seconds (see tables 7.5 and 7.6 and figure 7.2). The curves shown in figure 7.2 appear to converge as the window start time is increased. This behavior is to be expected since the sampling volumes are also more similar at 6.5 seconds than at 4.5. This is because the sampling ellipsoid for the deep data set becomes more hemispherical in shape at later lapse times since it's size increases while the distance between the foci (source and receiver) remains fixed. Thus, the sampling volumes are expected to converge with later and later window start times.

The slightly lower coda-Q for the shallow data set at the window start time of 4.5 seconds, and the greater similarity of the coda-Q values for the shallow and deep data sets at the start time of 6.5 seconds indicate that the average Q in the volcano and shallow crust is lower than in the deeper crust.

Values of the Q-Structure Model. Equation 5.1 was used to calculate values of the model parameters from observations of coda-Q at MSH (see chapter V). $Q_1(f)$ was calculated directly from the shallow data set using the earliest possible window start time (t_w) and shortest possible window, and hence the smallest possible sampling volume. The window was started at a lapse time of 1.0 sec and had a length of 3.5 sec. The frequency bands

Table 7.5 Coda from the shallow data set (6.5 sec). N is the number of bandpass filtered seismograms used to calculate the average Q at each f (Hz), and σ is the standard error of the mean.

Shallow Data Set 6.5 sec			
f	Q	σ	N
2	31	6.3	10
7	79	6.9	19
12	87	7.2	13
22	219	57.2	3

Table 7.6 Coda-Q from the deep data set (6.5 sec). N is the number of bandpass filtered seismograms used to calculate the average Q at each f (Hz), and σ is the standard error of the mean.

Deep Data Set 6.5 sec			
f	Q	σ	N
2	61	7.5	3
7	95	13.0	6
12	105	9.7	9
17	171	8.5	8
22	186	7.2	5
27	206	16.2	3

were overlapped slightly because a slight degree of overlapping tended to increase the number of Q_1 values to be averaged at each frequency. The 3.5 second window resulted in few Q_1 values with $\rho \geq 0.45$ except when the bands were slightly overlapped. The sampling volume corresponding to the window used has a radius of 4 km. Therefore a was chosen to be 4 km. It must be noted that this choice of a was determined by limitations in the data and the technique and does not necessarily represent the true radius of the low-Q volume at MSH. However, given that the size of the volcano itself is of the same order, 4 km seems a reasonable choice for a.

$Q_2(f)$ was determined indirectly by rearranging equation 5.1 as a function of R, $Q_1(f)$, a, and $Q(f, R)$. Values of $Q(f, R)$ were then calculated using a later window start time to sample a larger volume. The deep data set was used to calculate $Q(f, R)$ for this later t_w, since the duration of the seismograms in the deep data set is longer, which allows a larger sampling volume. The resulting values of the model parameters are shown in table 7.7 and figure 7.4. Note that the model was calculated using windows which include coda waves at lapse times between 2 and 15 sec. Also note that equation 5.1 holds only when $R > a$, or equivalently, when $t > 2a/v$. Therefore, the model is only valid for lapse times between $2a/v$ and 15 sec, where 15 sec corresponds to a sampling volume roughly 22 km in radius, assuming an S-wave velocity of 3 km/sec.

Discussion. The Q-structure which is indicated by the coda-Q results is an average structure which may be due to variations in $Q(f)$ with depth, variations in $Q(f)$ laterally, or both. Evidence for variation in Q with depth in western Washington was found by Zitek (1982). Assuming a frequency independent Q which varies only with depth, Zitek calculated an inverse model for Q (measured by the spectral ratio method) in the crust

Table 7.7 Values of the Q-structure model. f is in Hz.

Q-Structure Model		
f	Q_1	Q_2
2.0	10	123
6.0	67	99
10.0	128	149
14.0	140	175
18.0	153	251
22.0	156	607
26.0	162	3023

Table 7.8 Coda-Q values for Kilauea (Aki and Koyanagi, 1981). f is in Hz.

Kilauea	
f	Q
1.5	260
3.0	290
6.0	270
12.0	520

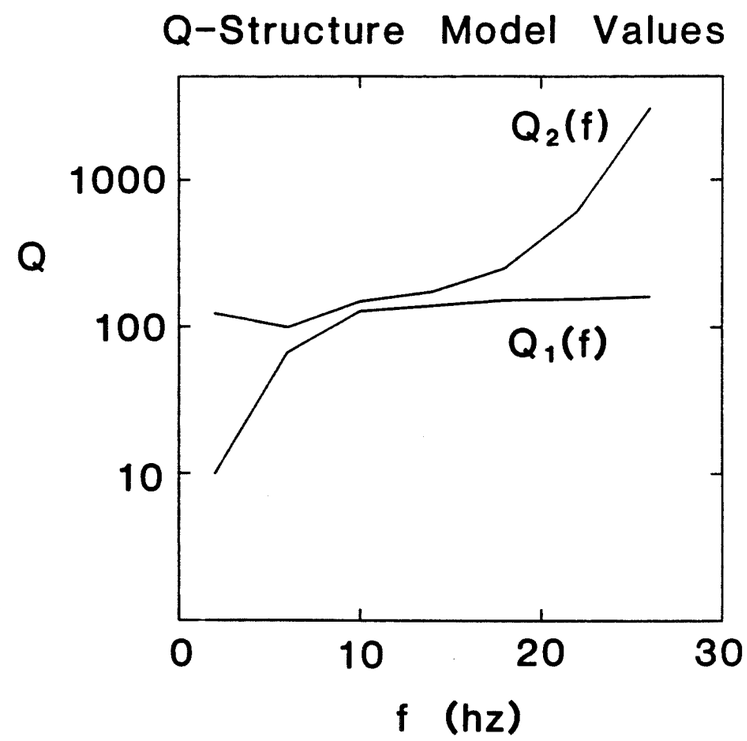

Figure 7.4 Values of the Q-structure model. f is frequency in Hertz. Upper curve is $Q_1(f)$ and lower curve is $Q_2(f)$.

and upper mantle of Western Washington (see figure 7.5). Note that Zitek's model shows a minimum Q at shallow depth, and an increase in Q with depth except for a marked decrease in Q at 25 to 35 km. The coda-Q values calculated by Havskov et al. (1987) represent the average $Q(f)$ in a sampling volume roughly 54 km in radius so that the structure shown in Zitek's model would be averaged by the coda-Q measurement. The coda-Q values calculated by Havskov et al. (1987) are consistent with Zitek's model since they are of the same order of magnitude. The resolution lengths and standard deviations for Zitek's model indicate that it is not reliable for depth's shallower than about 15 km. Thus, his model is not inconsistent with the coda-Q results which indicate that $Q(f)$ does vary with depth in the shallow crust at MSH.

There is no way to determine, from the data used in this analysis, what the Q values are for the volcano itself since a large fraction the smallest possible sampling volume probably includes rocks which are deeper and older than the volcano. It is possible, that the Q values for the volcano are much lower than the coda-Q values for this smallest sampling volume. Q_β for the volcano might be measured by using the spectral ratio method for S-waves which have shallow paths. The Q_β for the volcano may be lower than that for the region surrounding it. The low velocity rocks in the shallow volcanic structure probably have a lower intrinsic-Q (Q_i). I would expect Q_i for a young bed of volcanic ash to be lower than for a lithified bed of sedimentary rock since the ash would be more porous. The highly heterogeneous velocity structure of the volcano should produce a significant degree of scattering, causing the scattering-Q to be low (see equation 3.1). When the scale-length of the heterogeneities is comparable to the wavelength of the seismic waves interacting with it, then the effect of scattering is expected to be a maximum

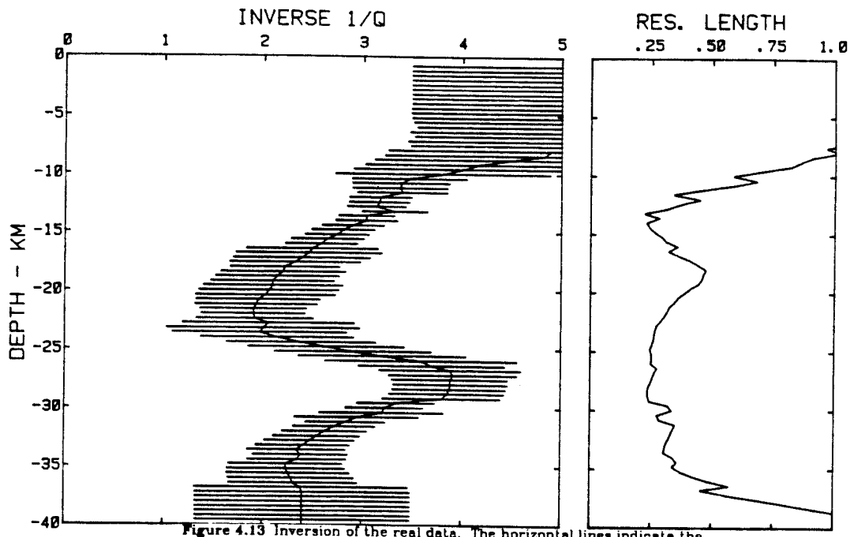

Figure 4.13 Inversion of the real data. The horizontal lines indicate the calculated data plus and minus two standard deviations. The scale of Q^{-1} is Q^{-1} times 10^{-3}. The resolution length should be multiplied by 40 km.

Figure 7.5 Zitek's model for depth-dependent Q. Shown above is an inverse model of frequency-independent Q in Western Washington (from Zitek, 1982). Plot at left is $1/Q$ vs. depth. At right is the resolution length vs. depth. Original caption provides additional details.

(Menke et. al., 1985; Aki and Richards, 1980). A reasonable mean shear velocity for shallow depths at the volcano is roughly 1.5 km/sec. The frequency band which is recorded by the University of Washington network at MSH is about 1 to 30 Hz. If the wave velocity v is equal to (λf) where λ is wavelength and f is frequency, then the wavelengths of the observed seismic waves are in the range 50 meters to 1.5 km. The scale-length of lava flows, dikes, and other volcanic features are comparable to this wavelength range. Therefore, it is reasonable to expect a significant degree of scattering within the volcano by heterogeneities, although it is impossible to say whether or not the degree of scattering would be lower (Q_s higher) in the surrounding crust.

Aki and Koyanagi (1981) calculated coda-Q values for Kilauea in Hawaii and these values are compared with those for the shallow data set at MSH in table 7.8 and figure 7.6. The Q values for Kilauea are about an order of magnitude higher than at MSH. However, Aki and Koyanagi do not provide error bars or lapse times so the corresponding sampling volume is not specified. Kilauea erupts basaltic lava while MSH erupts ash and lava ranging in composition from dacite to basalt. This compositional difference may partly explain the difference in the Q values. If the sampling volume for the Kilauea curve includes very deep rocks, then an increase in Q with depth will also contribute to the difference between the curves. Thus, the significantly higher Q at Kilauea doesn't necessarily indicate that Q at MSH is unusual.

If the volcano itself has a much lower Q than the shallow crust beneath it, then part of the "source depth effect" (see chapter II) is most likely due to the ascent of the seismic source from the deeper and higher Q rocks into the shallow low Q volcanic rocks. The medium and low frequency volcanic

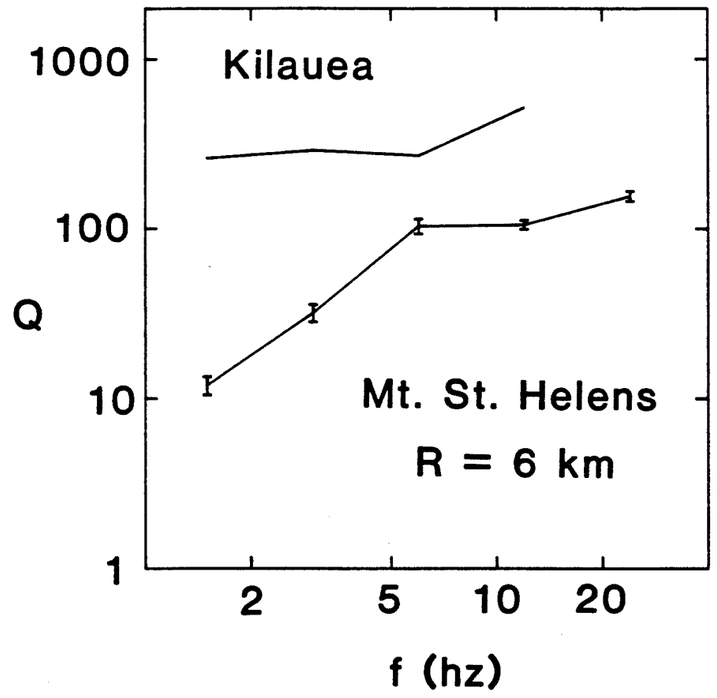

Figure 7.6 Coda-Q for Kilauea. Coda-Q for Mt. St. Helens is compared to coda-Q for Kilauea (Aki and Koyanagi, 1981). f is frequency in Hertz. Error bars on the MSH curve are one standard error of the mean. MSH curve corresponds to a sampling volume 6 km in radius. No error estimates or sampling volume details are available for the Kilauea curve.

earthquakes have sources which occur in the same depth range suggesting that changes in Q with depth are not the only cause of the differences between type (m) and (l) events. The Q-structure model is a model for the average structure. Since the coda is a superposition of many waves arriving from all directions then it is sensitive to this average structure. If we can use the model to remove the effect of attenuation from the coda then we can use the corrected coda to learn something about the source(s) of volcanic earthquakes. Assuming that the sources for type (m) and (l) events are different, then the corrected coda for a type (m) event should have different characteristics than that of a type (l) event.

CHAPTER VIII

CORRECTED SPECTRA OF VOLCANIC EARTHQUAKES

The model for spatial variation of Q at MSH, which was discussed in chapters V and VII, was used to attempt to separate the effects of the seismic source from the effects of attenuation on the seismograms of volcanic earthquakes. A convenient way to attempt the separation is by applying a correction for attenuation in the frequency domain. The Q-structure model was used to correct the spectra of the coda of volcanic seismograms. These corrected spectra were then compared with the uncorrected spectra at a series of lapse times.

For a fixed lapse time t, the spectrum of the coda is described by

$$A(f, t) = C(f)\, t^{-u}\, e^{-\pi f t/Q} \qquad (3.5).$$

The instrument response, $I(f)$, can be separated from $C(f)$ by rewriting 3.5 as,

$$A(f, t) = I(f)\, \sigma(f)\, t^{-u}\, e^{-\pi f t/Q} \qquad (8.1)$$

where $\sigma(f)$ includes the effects of the earthquake source, backscattering, and the station site, all of which are assumed independent of time. I will refer to $\sigma(f)$ as the "coda source spectrum". If $I(f)$ and Q are known, then observations of $A(f, t)$ can be used to determine $\sigma(f)$. At MSH the coda-Q results indicate that Q in equation 8.1 is a function of frequency and

position. As we saw in chapter V, Q is taken to have the form $Q(f, R)$.

There are several problems encountered when making the Q-correction. First, the fourier transform of the coda must be calculated at a fixed time to determine $A(f, t)$. The fourier transform will resolve only those frequencies which are higher than the inverse of the window length. To resolve lower frequencies it is necessary to use longer windows. The lowest frequency at which coda-Q was calculated in this study is 1.5 Hz, so that a spectral correction at lower frequencies is not possible. The values of the Q-structure model were calculated at distinct frequencies so it is necessary to interpolate to estimate the values of the Q-correction at intermediate frequencies. The values of the attenuation and geometrical spreading terms in equation 8.1 change with time since t explicitly appears in those terms. The value of $Q(f, R)$ will also change with time since $R = t\ v/2$ in equation 5.1. Therefore, over the length of any coda window, these quantities will change so that it is desirable to use the shortest possible window, to minimize their effects. Thus, the nature of the spectral correction involves a trade-off between using the shortest possible window and resolving the lower frequency spectral components.

In view of the above problems and complications related to applying the Q-correction, I used a window length of 2.56 sec. This length was used so that the values of the attenuation and geometrical spreading terms, which are calculated at the center of the window, are approximately correct over the entire window. In addition, 2.56 sec is long enough to allow adequate resolution of the spectral components with frequencies as low as about 0.5 Hz.

Spectral Results. The spectra for two types of volcanic seismograms (m and l) were corrected for attenuation using the Q-structure model. Both

earthquakes were located at shallow depth (< 1 km). The seismograms were recorded at station STD which is located on the flanks of the volcano, rather than in the crater. Therefore the assumption that the source and receiver are in the same location, which was used to derive equation 5.1, is violated. However, the distance between the sources and the receiver will be small relative to the the size of the sampling volume when the lapse times are large. This means that the assumption of a zero source-receiver separation will be better at later lapse times. Another problem with using this flank station is that there are likely to be surface waves in the coda to a greater degree than for stations in the crater. This is due to the low velocity materials in the shallow structure of the volcano and to the larger incident angles of the surfacing body waves for stations farther away from the epicenter.

The seismogram of the type (m) event and its spectra are shown in figure 8.1. The seismogram has an impulsive first arrival with a relatively high-frequency beginning and a low frequency coda. All of the spectra were corrected for instrument response to the extent that they can be - that is, they were corrected for the approximate shape of the instrument response since the details of the station response are not known. Each plot shows two spectra from the same coda window. One spectrum was corrected for attenuation and the other is uncorrected. The first spectral plot also includes a noise spectrum. The amplitudes of the coda spectra are comparable to the noise amplitudes for frequencies higher than about 20 Hz. The lowest frequency resolved by the fourier transform is about 0.5 Hz. Thus the spectra are only reliable in the band 0.5 to 20 Hz.

The spectra were calculated at a series of lapse times in the coda. The first spectral plot (a) is from a window starting at 1.0 sec, which is earlier than twice the S-wave travel time (t_s). Therefore, the first plot shows the

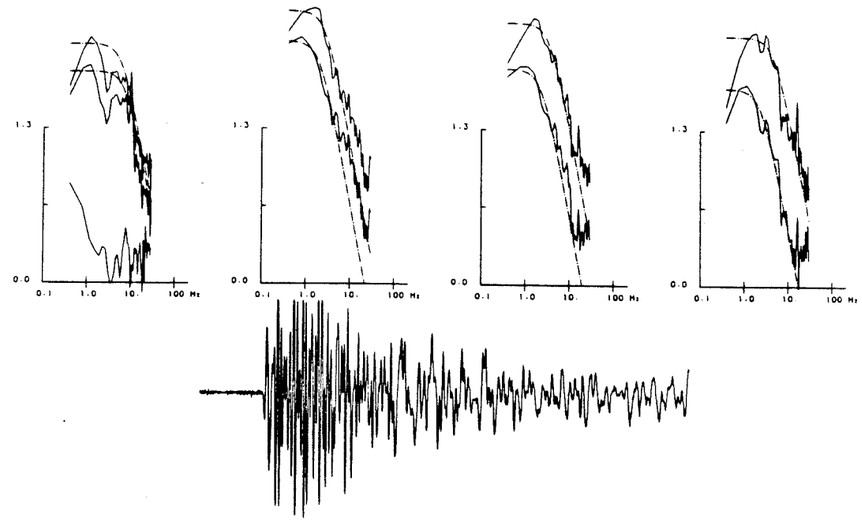

Figure 8.1 Corrected spectra of a type (m) seismogram. Spectra were corrected for attenuation using the MSH Q-structure model. Total length of seismic trace is 16.0 sec. Each plot corresponds to a different 2.56 sec long window of the trace as indicated. Windows are started as follows: *a* at 1.0 sec, *b* at 4 sec, *c* at 8 sec, and *d* at 12 sec. Noise spectrum is shown in plot *a*. Dashed curves are best-fit theoretical spectral envelopes.

spectrum of the direct waves. The subsequent plots were calculated after $2t_s$. Figure 8.1 shows that the uncorrected spectrum rapidly loses its high-frequency energy as the lapse time is increased. The appearance of the seismogram also clearly displays this behavior. In contrast, the corrected spectrum maintains its high-frequency energy, even at later lapse times. The relative invariance with time of the corrected spectrum compared to the uncorrected spectrum is consistent with the hypothesis that the corrected coda spectrum is the coda source spectrum, $\sigma(f)$, which is independent of time. These spectra suggest that the low frequency coda of this medium frequency seismogram is due to the particular Q-structure at MSH, rather than a source effect.

Another set of spectra were calculated from this type (m) event by using a model which assumes a homogeneous Q-structure. The coda-Q results at MSH do not support this type of model. If the effect of this model on the spectra of the type (m) seismogram is clearly unreasonable then it can be argued that the Q-structure at MSH is not homogeneous. The model was calculated using the shallow data set and the longest possible window which was 8 seconds and corresponds to a sampling volume about 9 km in radius. The spectra for the type (m) seismogram were corrected for attenuation using this model and they are illustrated in figure 8.2. The "corrected" spectrum increases drastically with lapse time suggesting that the homogeneous model is inappropriate for MSH.

The seismogram of the type (l) event and its spectra are shown in figure 8.3. The seismogram is very emergent and relatively low frequency throughout, except for a significant higher frequency noise component superposed on the low frequency signal. The spectra were corrected using the (heterogeneous) Q-structure model in the same way as those for the type (m)

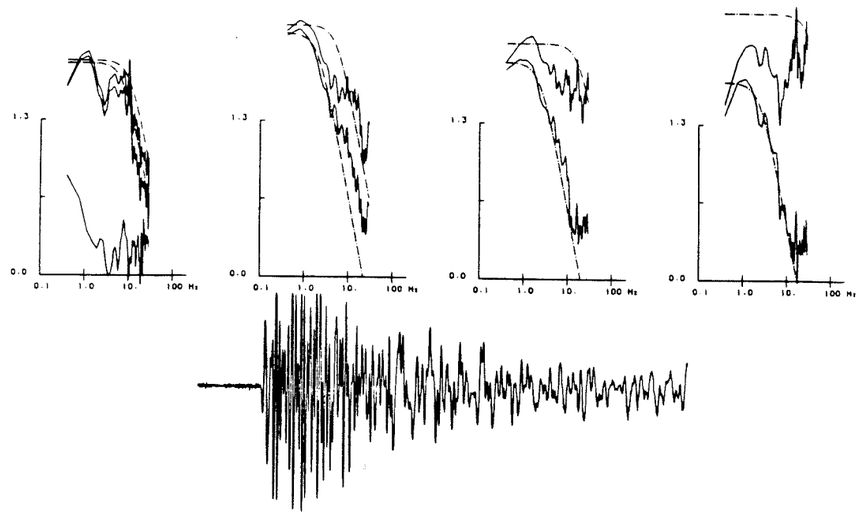

Figure 8.2 Corrected spectra assuming homogeneous Q-structure. Spectra of a type (m) seismogram are shown. Total length of seismic trace is 16.0 sec. Each plot corresponds to a different 2.56 sec long window of the trace as indicated. Windows are started as follows: *a* at 1.0 sec, *b* at 4 sec, *c* at 8 sec, and *d* at 12 sec. Noise spectrum is shown in plot *a*. Dashed curves are best-fit theoretical spectral envelopes.

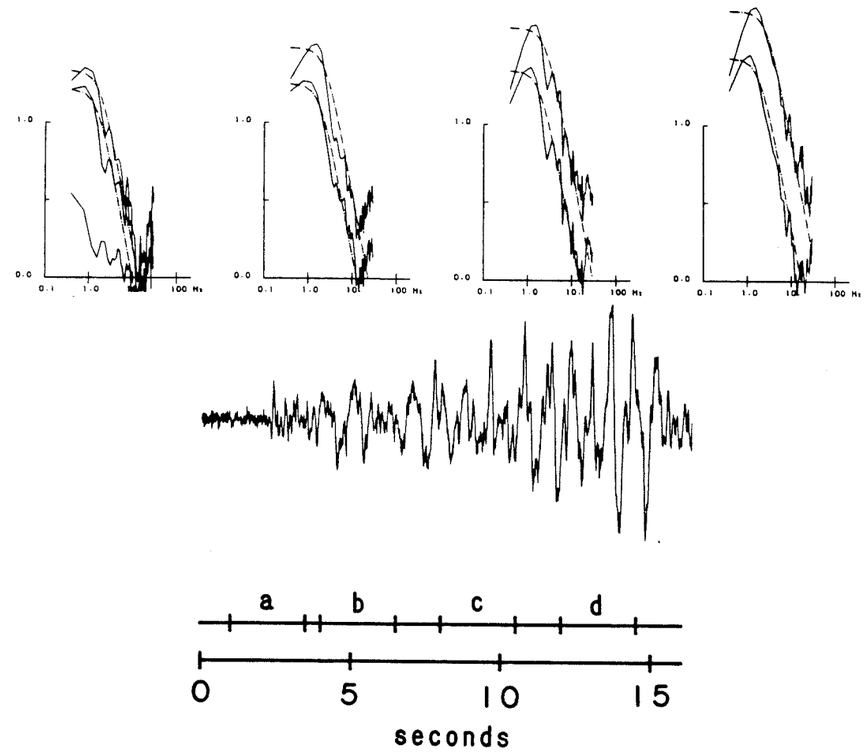

Figure 8.3 Corrected spectra of a type (l) seismogram. Spectra were corrected for attenuation using the MSH Q-structure model. Total length of seismic trace is 16.0 sec. Each plot corresponds to a different 2.56 sec long window of the trace as indicated. Windows are started as follows: *a* at 1.0 sec, *b* at 4 sec, *c* at 8 sec, and *d* at 12 sec. Noise spectrum is shown in plot *a*. Dashed curves are best-fit theoretical spectral envelopes.

event and are reliable in the same frequency band. The effect of lapse time on the spectra is similar to that for the type (m) spectra. However, there are two important differences. First, the uncorrected spectrum changes relatively little with lapse time suggesting that attenuation is not the only process producing the lower frequency waveform. Second, the corrected spectrum increases with lapse time. This suggests that the source for this earthquake is probably not of the tectonic type since the corrected spectrum (presumably the coda source spectrum) should not change with time. One possible type of source is one which radiates its characteristic spectrum over a long time scale, say several seconds. This could explain the invariance of the uncorrected spectrum with lapse time since the source would be feeding energy into the medium much longer than a typical tectonic source. Thus, the signal would not lose its high frequency energy with time because the source replenishes the energy which is dissipated by attenuation. The increase with time of the corrected spectrum is consistent with this hypothesis. The model for the coda of local earthquakes which was used to calculate coda-Q assumes a source duration that is short compared to the duration of the seismogram, so that, at a fixed frequency, the coda decay is only controlled by attenuation and geometrical spreading (see equation 3.5). If the source for this low frequency earthquake has a long duration, then the type of Q-correction being applied is inappropriate, and should be expected to cause the corrected spectrum to increase with time.

Conclusion

The above spectral observations are consistent with several statements about volcanic earthquakes at MSH. First, the medium frequency volcanic

earthquakes have a low frequency coda compared to a typical tectonic earthquake, but the characteristics of this coda can be accounted for by the Q-structure at MSH rather than a non-tectonic source. Second, the low frequency volcanic earthquakes have a source which is rather different than a typical tectonic source, at least in terms of source duration. Third, the Q-structure at MSH is not homogeneous and this statement is supported by the coda-Q results.

BIBLIOGRAPHY

Aki, K. (1969). Analysis of the seismic coda of local earthquakes as scattered waves, *J. Geophys. Res.,* **74,** 615-631.

Aki, K. (1980). Attenuation of shear waves in the lithosphere for frequencies from 0.05 to 25 Hz, *Phys. Earth Planet Interiors,* **21,** 50-60.

Aki, K. (1981). Attenuation and scattering of short-period seismic waves in the lithosphere, *Identification of seismic sources - earthquakes or underground explosions,* E. S. Husebye and S. Mykkeltweit, editors, D. Reidel Publishing Co., Dordrecht, The Nederlands.

Aki, K. and B. Chouet (1975). Origin of coda waves: source, attenuation, and scattering effects, *J. Geophys. Res.,* **80,** 3322-3342.

Aki, K. and R. Koyanagi (1981). Deep volcanic tremor and magma ascent mechanism under Kilauea, Hawaii, *J. Geophys. Res.,* **86,** 7095-7109.

Aki, K. and P. G. Richards (1980), *Quantitative Seismology,* W. H. Freeman and Company, San Francisco, CA.

Aki, K., M. Fehler, and S. Das (1977). Source mechanism of volcanic tremor: Fluid-driven crack models and their application to the 1963 Kilauea eruption, *J. Volcanol. Geotherm. Res.,* **2,** 259-287.

Bakun, W. H. and C. G. Bufe (1975). Shear-wave attenuation along the San Andreas Fault zone in central California, *Bull. Seismol. Soc. Amer.,* **65,** 5439-5459.

Bevington, P. R. (1969). *Data Reduction and Error Analysis for the Physical Sciences,* McGraw-Hill, Inc., New York, NY.

Capon, J. (1969). High-resolution frequency-wave number spectrum analysis, *Proc. IEEE,* **57,** 1408-1419.

Chouet, B. (1985). Excitation of a buried magmatic pipe: a seismic source model for volcanic tremor, *J. Geophys. Res.,* **90,** 1881-1893.

Crosson, R. S. (1972). Small earthquakes, structure, and tectonics of the Puget Sound region, *Bull. Seismol. Soc. Amer.,* **62,** 1133-1171.

Crosson, R. S. and D. A. Bame (1985). A spherical source model for low frequency volcanic earthquakes, *J. Geophys. Res.,* **90,** 10,237-10,247.

Dainty, A. M. (1981). A scattering model to explain seismic Q observations in the lithosphere between 1 and 30 Hz, *Geophys. Res. Letters,* **8,** 1126-1128.

Dainty, A. M. and M. N. Toksoz (1977). Elastic wave scattering in a highly scattering medium - A diffusion approach, *J. Geophys. Res.,* **43,** 375-388.

Fehler, M. and B. Chouet (1982). Operation of a digital seismic network on Mt. St. Helens volcano and observations of long period seismic events that originate under the volcano, *Geophys. Res. Letters,* **9,** 1017-1020.

Gao, L. S., L. C. Lee, N. N. Biswas, and K. Aki (1983). Comparison of the effects between single and multiple scattering on coda waves for local earthquakes, *Bull. Seismol. Soc. Amer.,* **73,** 377-389.

Havskov, J., R. S. Crosson, S. D. Malone, and D. C. McClurg (1987). Coda-Q of the State of Washington, *Preprint.*

Herraiz, K. and A. F. Espinosa (1986). Scattering and Attenuation of High-Frequency Seismic Waves: Development of the Theory of Coda Waves, *U.S.G.S. Open File Report,* 86-455.

Kvamme, L. B. (1985). Attenuation of seismic energy from local events in Norwegian areas, *Cand. Scient. thesis,* Seismological Observatory, University of Bergen, Norway.

Malone, S. D. (1983). Volcanic earthquakes: Examples from Mt. St. Helens, *Earthquakes: Observations, theory, and interpretation, H. Kanamori, editor,* North Holland Publishing Co., Amsterdam.

Malone, S. D., C. Boyko, and C. S. Weaver (1983). Seismic precursors to the Mt. St. Helens eruptions in 1981 and 1982, *Science,* **229,** 1376-1378.

Malone, S. D. and A. Qamar (1985). Repetitive Microearthquakes as the source for volcanic tremor at Mt. St. Helens (abstract), *EOS Trans. AGU,* **65,** 1001.

McNutt, S. R. (1986). Observations and analysis of B-type earthquakes, explosions, and volcanic tremor at Pavlof volcano, Alaska, *Bull. Seismol. Soc. Amer.,* **76,** 153-175.

Menke, W., D. Witte, and R. Chen (1985). Laboratory rest of apparent attenuation formulas, *Bull. Seismol. Soc. Amer.,* **75,** 1383-1393.

Minakami, T. (1960). Fundamental research for predicting volcanic eruptions (I)-Earthquakes and crustal deformations originating from volcanic activities, *Bull. Earthquake Res. Inst., Tokyo Univ.,* **38,** 497-544.

Mullineaux, D. R. and D. R. Crandell (1981). The eruptive history of Mt. St. Helens, *U.S.G.S. Prof. Paper,* **1250,** 3-15.

Phillips, W. S., W. H. K. Lee, and J. T. Newberry (1986). Spatial variation of crustal coda-Q in California, *Preprint.*

Pulli, J. J. (1984). Attenuation of coda waves in New England, *Bull. Seismol. Soc. Amer.,* **74,** 1149-1166.

Rautian, T. G. and V. I. Khalturin (1978). The use of the coda for determination of the earthquake source spectrum, *Bull. Seismol. Soc. Amer.,* **68,** 923-948.

Sato, H. (1977). Energy propagation including scattering effects: single isotropic scattering approximation, *J. Phys. Earth,* **25,** 27-41.

St. Lawrence, W. and A. Qamar (1979). Hydraulic transients: A seismic source in volcanoes and glaciers, *Science,* **203,** 654-656.

Weaver, C. S. (1976). Seismic events on Cascade volcanoes, *Ph.D. dissertation,* University of Washington.

Weaver, C. S. and S. D. Malone (1976). Mount St. Helens seismic events: volcanic earthquakes or glacial noises?, *Geophys. Res. Letters,* **3,** 197.

Weaver, C. S., W. C. Grant, S. D. Malone, and E. T. Endo (1981). Post-May 18 seismicity at Mt. St. Helens: volcanic and tectonic implications, *U.S.G.S Prof. Paper,* **1250,** 109-121.

Zitek, W. O. (1982). A study of inverse-Q as a function of depth in western Washington, *Master's thesis,* University of Washington.